Volume 20 | Number 23 | 21 June 2018 | Pages 3123–3268

CrystEngComm

rsc.li/crystengcomm

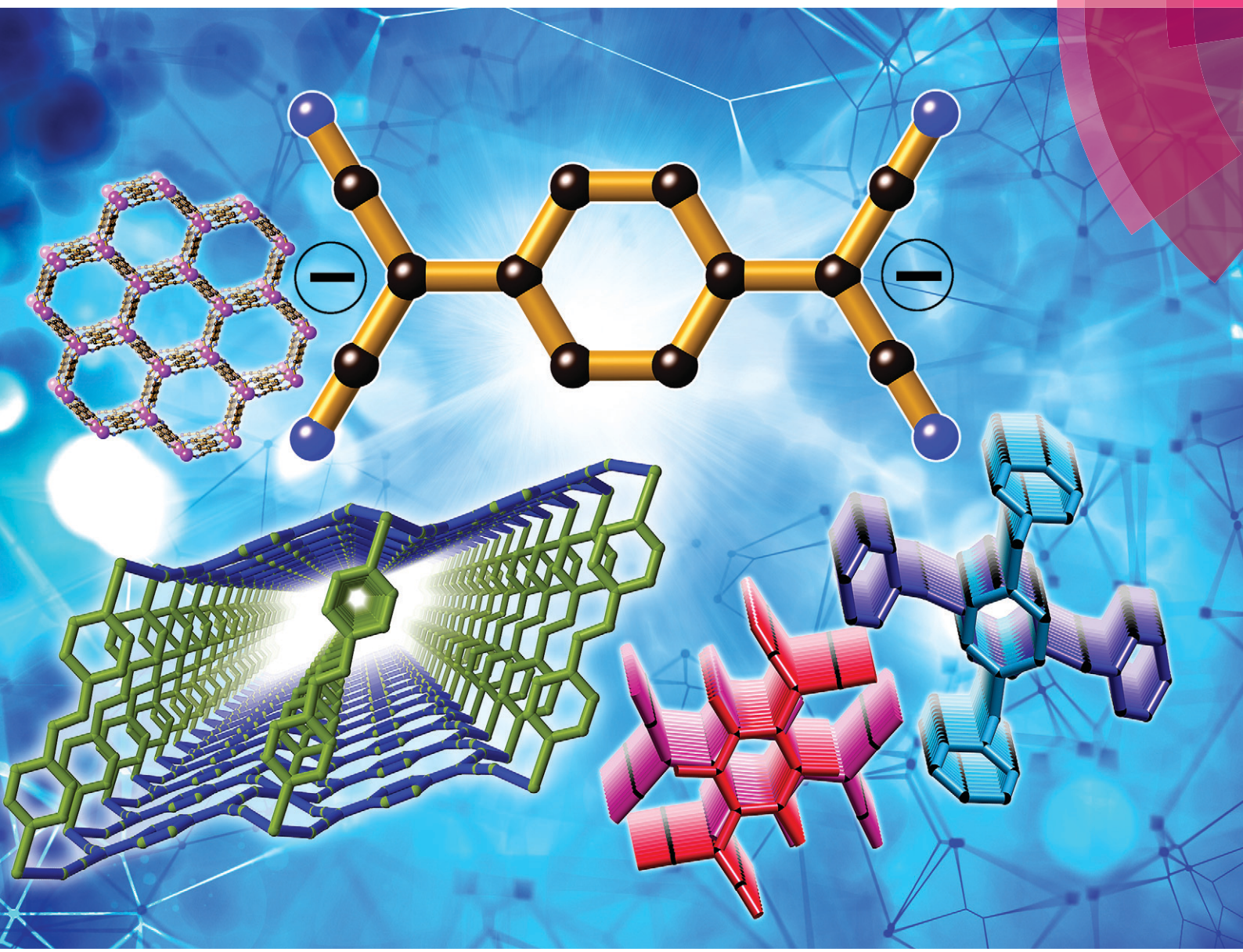

ROYAL SOCIETY OF CHEMISTRY

HIGHLIGHT

Brendan F. Abrahams, Richard Robson *et al.*

X_4TCNQ^{2-} dianions: versatile building blocks for supramolecular systems

CrystEngComm

HIGHLIGHT

View Article Online
View Journal | View Issue

Cite this: *CrystEngComm*, 2018, **20**, 3131

X_4TCNQ^{2-} dianions: versatile building blocks for supramolecular systems

Brendan F. Abrahams, * Robert W. Elliott, Timothy A. Hudson, Richard Robson* and Ashley L. Sutton

Received 17th March 2018,
Accepted 11th April 2018

DOI: 10.1039/c8ce00413g

rsc.li/crystengcomm

In 2008 a new approach to generating tetracyanoquinodimethane (TCNQ)-based materials was described which involved the use of the diprotonated, reduced form of TCNQ ($TCNQH_2$) as a reactant. Since the initial work, the dianionic forms of $TCNQH_2$ and F_4TCNQH_2 have been incorporated into a wide assortment of co-ordination polymers in which the ligand, with four potential donor atoms, binds to a variety of metal centres. The structures of neutral 1D, 2D and 3D coordination polymers are described, in addition to the structures of anionic networks. Not surprisingly, the oxidation state of the metal ion as well as its preference for certain coordination geometries has a major influence upon the topology and geometry of the polymeric material. In addition to the identity of the metal centre, the type of structure obtained depends upon the nature of the co-ligand in the case of neutral polymers. For anionic networks the shape, charge and size of the counter-cation impacts upon the network connectivity. The large number of metal compounds formed with the dianions is in contrast with the relatively small number of metal complexes involving TCNQ and F_4TCNQ in the 0 and −1 oxidation states. In addition to coordination polymers, organic salts of $TCNQ^{2-}$ and F_4TCNQ^{2-} have also been investigated. The packing within these crystalline salts has been categorised into four types. In both the case of the coordination polymers and the organic salts, charge transfer interactions are common with the electron-rich $TCNQ^{2-}$ and F_4TCNQ^{2-} dianions often serving as electron donors. The presence of various species in the crystal that can act as electron acceptors normally leads to intensely coloured crystals. Whilst $TCNQ^{2-}$ and F_4TCNQ^{2-} dianions have been shown to be versatile building blocks capable of yielding a variety of unusual and aesthetically appealing structures, the redox activity of these dianions offers the prospect of creating materials that possess fascinating electronic properties. An overview of the types of structures obtained since 2008 using the $TCNQH_2/F_4TCNQH_2$ synthetic approach is presented.

Introduction

Over the last fifty years there has been considerable interest in tetracyanoquinodimethane (TCNQ, **I**, X = H) and its derivatives because their presence in both inorganic and organic materials leads to interesting magnetic and electronic properties.[1–3] The charge transfer complex, TTF–TCNQ, is widely regarded as the first "organic metal" (TTF = tetrathiafulvalene).[4–6] Although the complex is formally a semi-conductor, it exhibits a level of conductivity comparable to that of metal conductors. The interesting physical properties commonly found with TCNQ complexes are associated with the ready accessibility of the relatively stable radical anionic state, $TCNQ^{\bullet-}$ (**II**). Whilst TCNQ is able to exist, unambiguously, as both a neutral molecule and a monoanionic radical, mixed valence states are common.[1,2,7] For example, in the aforementioned charge transfer complex, TTF–TCNQ, in which TCNQ is considered to be an electron acceptor and TTF an electron donor, the charge on the TCNQ has been calculated to be −0.59 whilst the TTF carries a positive charge of the same magnitude.[8] There is a sizeable structural library of organic TCNQ-based compounds within the literature, many of which involve some form of charge transfer. In the vast majority of cases in which the radical monoanion is present, it exists as π-dimers, $(TCNQ^{\bullet-})_2$ or conglomerates comprised of $TCNQ^{\bullet-}$ and TCNQ units.

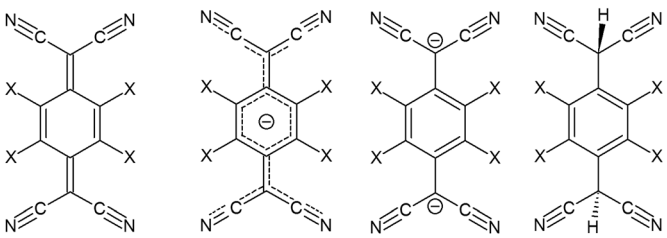

I **II** **III** **IV**

TCNQ has four *N*-donor atoms directed towards the vertices of a rectangle and thus it offers the prospect of acting as

School of Chemistry, University of Melbourne, Parkville, Victoria 3010, Australia. E-mail: bfa@unimelb.edu.au, r.robson@unimelb.edu.au; Fax: +61 3347 5180

a ligand in the formation of discrete and polymeric metal complexes. The first structurally characterised radical-derived coordination polymer, $Ag^{I}TCNQ^{\bullet-}$, was reported by Shields[9] and consists of two independent interpenetrating 3D networks. In this structure, both the Ag(I) centres and the $TCNQ^{\bullet-}$ ligands serve as 4-connecting nodes within a 3D network which possesses the PtS topology; the Ag(I) centre and the $TCNQ^{\bullet-}$ unit correspond to the tetrahedral S^{2-} anion and the planar 4-connecting Pt^{2+} cation respectively. Dunbar and co-workers later described two semi-conducting forms (phase I and II) of CuTCNQ.[10] The crystal structure of the interpenetrating phase I shows close contacts between $TCNQ^{\bullet-}$ units in neighbouring networks, whereas phase II possesses a 3D structure with a distinctly different topology. AgTCNQ, CuTCNQ phase II and some substituted derivatives have been investigated as candidates for electronic devices due to their resistance-state switching,[11–17] field emission[18–20] and optical properties.[21–24]

Whilst there has been considerable interest in the generation of metal–$TCNQ^{\bullet-}$ compounds[25–38] there are surprisingly few examples of structurally characterised extended framework materials in the literature[39–56] with many of the compounds being inhomogeneous and exhibiting poor crystallinity.[43,57–66] As an example, the family of compounds formulated as $M^{II}(TCNQ)_n$ (M^{II} = Mn, Fe, Co, Ni) were found to display interesting magnetic behaviours at low temperatures, however the exact composition of the materials is unclear.[61] In the 1990's we undertook synthetic investigations with the aim of producing novel metal–TCNQ coordination polymers, however, after failing to produce the targeted compounds we abandoned this area. We suspect that other workers in this area may have had similar experiences in trying to incorporate the radical form of TCNQ into coordination networks.

The two-electron reduction of X_4TCNQ (**I**) generates the spin-paired dianion, X_4TCNQ^{2-} (**III**), which possesses an aromatic core. In contrast to the neutral and radical forms, which are π-acceptors, the dianion is a π-donor. Siedle *et al.* reported air-sensitive transition metal derivatives of the TCNQ dianion in 1979.[67] These almost black compounds, which were not structurally characterised, were obtained by the reduction of neutral TCNQ with organometallic species. In 2006 the structures of divanadium–$TCNQ^{2-}$ complexes were reported by Choukroun and co-workers[68] and in the same year Kitagawa *et al.* reported a coordination network in which neutral parallel 2D sheets of composition Zn(TCNQ) are linked by 4,4′-bipyridine to form a beautiful 3D network containing solvent-filled voids.[69] In the paper reporting this structure the authors suggest that the dianionic form of TCNQ is a product from the disproportionation of the radical monoanion, $TCNQ^{\bullet-}$. Dunbar and co-workers also proposed that the disproportionation of $F_4TCNQ^{\bullet-}$ led to the formation of F_4TCNQ^{2-} which served as a bridging ligand within a Mn(II) coordination network.[70] The first structurally characterised compound, involving the uncoordinated $TCNQ^{2-}$ dianion was the charge transfer salt $[Co^{III}(C_5Me_5)_2]_2$-(TCNQ), obtained *via* the reduction of TCNQ, which was reported in 1987.[71]

The TCNQ and F_4TCNQ dianions have the potential to participate in charge transfer interactions with suitable acceptors. The electron rich X_4TCNQ dianions are colourless in the absence of an acceptor but when combined with appropriate electron acceptors the resulting charge transfer complexes are often intensely coloured. The compounds reported in this highlight range from colourless to black, indicating various degrees of charge transfer.

Up until 2008 there were relatively few examples of crystal structures incorporating X_4TCNQ in its dianionic form.[68–70,72,73] In each case the dianion was formed either *via in situ* reduction of TCNQ or $TCNQ^{\bullet-}$ or the disproportionation of the radical anion. Whilst the dianion, X_4TCNQ^{2-}, readily undergoes oxidation, its doubly protonated form, X_4TCNQH_2 (**IV**), is much more stable and far easier to handle.[74] In 2008 we proposed that it may be possible to generate TCNQ-based coordination networks in which metal centres are linked by the dianion, by combining $TCNQH_2$ with metal ions in the presence of a weak base.[75] This work succeeded in demonstrating that although the dianion is susceptible to reaction with oxygen,[76] it can be stabilised by coordination to metal centres. In addition, by starting with $TCNQH_2$ it has been shown that the dianion can be stabilised in the presence of appropriate counter-cations.[75] Similar work with F_4TCNQ^{2-} has resulted in analogous products.

The redox activity of TCNQ and F_4TCNQ has been studied using cyclic voltammetry.[74] Two reversible, one-electron couples were found for TCNQ as indicated:

$$E^{\circ}(vs.\ Ag/Ag^{+})$$

$$TCNQ + e^{-} \rightarrow TCNQ^{\bullet-} \quad -0.05\ V$$

$$TCNQ^{\bullet-} + e^{-} \rightarrow TCNQ^{2-} \quad -0.59\ V$$

Similar reversible reduction processes occur for F_4TCNQ, however the reduction potentials are each shifted ~0.36 V to higher potentials as a result of the electron withdrawing F atoms providing stabilisation of the anionic forms.

$$E^{\circ}(vs.\ Ag/Ag^{+})$$

$$F_4TCNQ + e^{-} \rightarrow F_4TCNQ^{\bullet-} \quad 0.31\ V$$

$$F_4TCNQ^{\bullet-} + e^{-} \rightarrow F_4TCNQ^{2-} \quad -0.22\ V$$

These data indicate that $TCNQ^{2-}$ is more easily oxidised than F_4TCNQ^{2-} and in general it has been found in synthetic investigations that compounds involving the fluorinated dianion are more stable upon exposure to the atmosphere.

Nevertheless, compounds involving either type of dianion exhibit reasonable stability either upon coordination to metal centres or in the formation of charge–transfer complexes.

Since our initial work in 2008 we have employed X_4TCNQH_2 (X = H, F) (**IV**) in the synthesis of a wide range of novel materials that incorporate the dianionic species, X_4TCNQ^{2-}. The use of the acid form represents a new synthetic approach in the generation of crystalline X_4TCNQ-based compounds. It was anticipated that the increased negative charge on the anion, relative to the radical monoanion form, would allow the ligands to bind more strongly to metal centres thus yielding more robust networks. Thus far, X_4TCNQ^{2-} has shown a propensity to form coordination polymers in which face-to-face intra-framework TCNQ–TCNQ interactions are not common, which is presumably a consequence of electrostatic repulsion associated with the formal charge of each $TCNQ^{2-}$ unit. One of our longer term aims is to intercalate oxidants into porous X_4TCNQ^{2-}-networks in order to generate mixtures of $X_4TCNQ^{0/-1/-2}$ oxidation states. The presence of intra-framework voids, in which one or both sides of the ligand is accessible, makes this an eminently reasonable objective. In this regard, we note that Dunbar and co-workers have reported the compound $[Cd_2(TCNQ)_{3.5}H_2O]$, which contains TCNQ in a variety of oxidation states from −0.66 to −1.57 (ref. 77) and also the compound $[M(TCNQ)_2(4,4bipy)(MeOH)_2]\cdot TCNQ\cdot 0.5H_2O$ (M = Mn, Zn), in which the TCNQ species have a charge of −2/3.[51]

This highlight is a structural review describing our recent work using the X_4TCNQH_2 synthetic approach, which has resulted in a series of crystalline compounds including:

1) Electrically neutral coordination polymers of general formula $[(M^{y+})_a(X_4TCNQ^{2-})_b(\text{co-ligand})_c]$, wherein the choice of metal centre and co-ligand has a marked effect on the network geometry and topology (Table 1);

2) Anionic coordination polymers of general formula $[(M^{y+})_a(X_4TCNQ^{2-})_b]^{z-}$ in which the counter-cation plays a crucial structure directing role and (Table 1);

3) Organic charge transfer salts of X_4TCNQ^{2-} (Table 2).

1. Electrically neutral coordination polymers

This section describes two types of coordination polymers. The first type includes networks in which divalent metal ions are linked by X_4TCNQ^{2-} ligands and the second type focuses solely on neutral Cu(I) coordination polymers.

Neutral coordination polymers with divalent metal centres

The 1 : 1 combination of a 4-coordinate TCNQ dianion with divalent metal centres within a network may be expected to yield metal centres in which a maximum of four coordination sites of the metal centre are occupied. Given that divalent metal centres often prefer higher coordination numbers, there is the possibility of introducing neutral co-ligands that can occupy additional coordination sites around the metal centre. As indicated by the examples presented below, the nature of the co-ligand has been found to have a major impact on the topology and geometry of the resulting structure. A range of structures are described in which a variety of co-ligands have been employed to generate 1D, 2D and 3D coordination polymers.

1D coordination polymers (**1–6**) have been formed in cases where some of the N atoms of the X_4TCNQ dianionic ligands are uncoordinated. The combination of $TCNQ^{2-}$ with Mn(II) and the bidentate co-ligand ethylenediamine (en) results in the formation of the 1D chain-like polymer, $[Mn(TCNQ)(en)_2]$ (**1**), wherein the $TCNQ^{2-}$ anion coordinates to two Mn^{II} centres through nitrile groups on opposite sides of the aromatic ring. Each metal centre is bound by two $TCNQ^{2-}$ units in a *cis* arrangement (Fig. 1a). When F_4TCNQ^{2-} is employed under similar reaction conditions, the metal centres are bound to the ligands by nitriles from the same $-C(CN)_2$ unit, with each Mn(II) centre coordinated by two F_4TCNQ^{2-} ligands in a *trans* fashion (**2**). The resulting linear polymers interdigitate, as shown in Fig. 1b. Compound **3**, $[Zn(F_4TCNQ)(2,2bipy)_2]\cdot MeOH$, adopts a structure with similar connectivity to that of **1**.

Linear "double-layered" polymers can be formed when $TCNQ^{2-}$ ligands bind to three metal centres. The compounds $[Cd(F_4TCNQ)(TACN)]$ (**4**) and $[Zn(F_4TCNQ)(TACN)]$ (**5**) have a 1D chain-like polymer in which the F_4TCNQ^{2-} ligand is bound to three metal centres whilst the octahedral metal centre is coordinated by three F_4TCNQ^{2-} anions and a 1,4,7-triazacyclononane (TACN) ligand in a *fac* arrangement (Fig. 1c). The compound $[Zn(F_4TCNQ)(2,2bipy)(MeOH)]$ (**6**) displays the same double layered strip motif as **4** and **5** but with a bidentate 2,2′-bipyridine (2,2bipy) ligand and a coordinated methanol molecule in place of the tridentate TACN ligand. In this case the non-coordinated nitrile group of the F_4TCNQ^{2-} ligand forms a hydrogen bond to a coordinated methanol molecule from an adjacent strip, leading to a 2D hydrogen bonded network (Fig. 1d).

A series of electrically neutral 2D coordination polymers with the general formula $[M^{II}(X_4TCNQ^{-II})(\text{co-ligand})_2]\cdot\text{solvate}$ have been structurally characterised (**7–25**). In the majority of cases, the X_4TCNQ^{2-} ligand is coordinated to four metal centres and each metal centre is bound to four X_4TCNQ^{2-} anions, to give a network which has the topology of a 4,4-net *i.e.* both the metal centres and the X_4TCNQ^{2-} ligands serve as four connecting nodes and the smallest circuit in the net contains four nodes. The octahedral metal centres are also coordinated by co-ligands which sit above and/or below the sheets. Two types of connectivity are observed within the sheets, wherein the $C–X_4C_6–C$ axes are either: i) alternating in orientation (type A), with a square-type array of metal centres of edge ~8.5 Å (Fig. 2a), or ii) parallel (type B), with the metal centres sitting at the corners of a rectangle of long edge ~11.3 Å and short edge ~7.4 Å (Fig. 2b). Due to the steric effects of the fluorine atoms, networks involving F_4TCNQ^{2-}, thus far, have only been found to adopt the type B arrangement.

Table 1 A selection of coordination polymers derived from X_4TCNQ^{2-}

Compound	Cp'd no.	CSD ref code	Colour	Type
$[Mn(TCNQ)(en)_2]$	**1**	DACCES	Colourless	1D
$[Mn(F_4TCNQ)(en)_2]$	**2**	DABLUQ	Orange	1D
$[Zn(F_4TCNQ)(2,2bipy)_2]\cdot MeOH$	**3**	DABXOW	Orange	1D
$[Cd(F_4TCNQ)(TACN)]\cdot MeOH$	**4**	DABXIQ	Yellow	1D double layer
$[Zn(F_4TCNQ)(TACN)]\cdot MeOH$	**5**	DABLOK	Yellow	1D double layer
$[Zn(F_4TCNQ)(2,2bipy)(MeOH)]$	**6**	DABMAX	Yellow	1D double layer
$[Zn_3(TCNQ)_3(MeOH)_5(DMF)]\cdot MeOH\cdot 3DMF$	**7**	CUTFII	Yellow	2D
$[Mn_3(TCNQ)_3(MeOH)_5(DMF)]\cdot 1MeOH\cdot 3DMF$	**8**	CUTCAX	Colourless	2D
$[Zn(TCNQ)(DMSO)_2]\cdot 0.41pyrazine\cdot \frac{1}{2}MeOH$	**9**	CUTDIG	Orange	2D
$Mn(F_4TCNQ)(DMSO)_2]\cdot pyz$	**10**	CUTBUQ	Pale yellow	2D
$[Mn(F_4TCNQ)(MeOH)_2]\cdot \frac{1}{2}(tmpyz)\cdot 1\frac{1}{2}(MeOH)$	**11**	CUTMOV	Yellow	2D H-bonding
$[Zn(F_4TCNQ)(MeOH)_2]\cdot Me_2pyz$	**12**	CUTDOM	Yellow	2D H-bonding
$[Zn(TCNQ)(MeOH)_2]\cdot tmpyz$ (1)	**13**	CUTDUS01	Orange	2D H-bonding
$[Zn(TCNQ)(MeOH)_2]\cdot tmpyz$ (1)	**14**	CUTDUS	Yellow	2D H-bonding
$[Cd(TCNQ)(MeOH)_2]\cdot tmpyz$	**15**	CUSZUN	Yellow	2D H-bonding
$[Mn(F_4TCNQ)(MeOH)_2]\cdot phenazine$	**16**	CUTCIF	Red/orange	2D H-bonding
$[Mn(F_4TCNQ)(MeOH)_2]\cdot 2acridine$	**17**	CUTCEB	Light orange	2D
$[Zn(TCNQ)(pyridine)_2]\cdot \frac{1}{2}MeOH$	**18**	QUQQAV	Colourless	2D interdigitating
$[Co(TCNQ)(quinoline)_2]\cdot DMF$	**19**	NAJGEM	Green	2D interdigitating
$[Zn(TCNQ)(quinoline)_2]\cdot DMF$	**20**	QUQQEZ	Green	2D interdigitating
$[Zn(TCNQ)(4\text{-phenylpyridine})_2]\cdot 2MeOH$ (2)	**21**	QUQQID	Pink	2D interdigitating
$[Zn(TCNQ)(4\text{-phenylpyridine})_2]$ (2a)	**22**	CUTFEE	Orange	2D interdigitating
$[Mn(TCNQ)(pyridine)_2]\cdot 2MeOH$	**23**	QUQQUP	Purple	2D interdigitating
$[Cd(TCNQ)(4\text{-picoline})_2]\cdot 2MeOH$	**24**	QUQRAW	Colourless	2D interdigitating
$[Zn(TCNQ)(nicotinamide)_2]\cdot DMF$	**25**	QUQQOJ	Pale yellow	2D H-bonding
$[Cd(F_4TCNQ)(DMSO)_2]$	**26**	DABMEB	Colourless	3D
$[Cd(TCNQ)(2,2bipy)]\cdot DMF$	**27**	SUMTUR	Light orange	2D corrugated
$[Mn(TCNQ)(2,2bipy)]\cdot DMF$	**28**	SUMVAZ	Light orange	2D corrugated
$[Mn(F_4TCNQ)(2,2bipy)]$	**29**	CUTBAW	Orange	2D corrugated
$[Mn(F_4TCNQ)(2,2bipy)]\cdot \frac{1}{2}(2,2bipy)$	**30**	CUSZOH	Yellow	2D corrugated
$[Cd(TCNQ)(phen)]\cdot DMF$	**31**	SUMVED	Yellow/orange	2D corrugated
$[Mn(TCNQ)(phen)]\cdot DMF$	**32**	SUNJOC	Yellow/orange	2D corrugated
$[Cd(F_4TCNQ)(phen)]$	**33**	CUTMEL	Orange	2D corrugated
$[Zn(F_4TCNQ)(phen)]\cdot \frac{1}{2}H_2O$	**34**	CUTFOO	Yellow	2D interdigitating
$[Co(TCNQ)(phen)]$	**35**	SUMVIH	Purple	3D
$[Fe(TCNQ)(4,4bipy)]\cdot solvate$	**36**	NAJFOV	Red	3D pillared
$[Co(TCNQ)(4,4bipy)]\cdot solvate$	**37**	NAJFUB	Red	3D pillared
$[Cd(TCNQ)(4,4bipy)]\cdot solvate$	**38**	NAJGAI	Yellow	3D pillared
$[Zn(TCNQ)(4,4bipy)]\cdot solvate$	**39**	VACJEQ	Yellow	3D pillared
$[Mn(TCNQ)(4,4bipy)]\cdot solvate$	**40**	QUQPEY	Yellow	3D pillared
$[Cd(TCNQ)(bpe)]\cdot solvate$	**41**	QUQPIC	Orange	3D pillared
$[Zn(TCNQ)(bpe)]\cdot solvate$	**42**	QUQPOI	Orange	3D pillared
$[Zn(TCNQ)(Obip)_1(MeOH)]\cdot DMF$	**43**	QUQPUO	Red	3D pillared
$[Cu^I_2(TCNQ)(2\text{-picoline})_2]\cdot EtOH$	**44**	BUKDOC	Colourless	1D
$[Cu^I_2(TCNQ)(isoquinoline)_2]$	**45**	BUKDUI	Pale yellow	1D
$[Cu^I_2(TCNQ)(4\text{-phenylpyridine})_2]$	**46**	BUKFAQ	Colourless	1D
$[Cu^I_2(F_4TCNQ)(2\text{-picoline})_2]\cdot MeCN$	**47**	BUKFEU	Pale yellow	1D
$[Cu^I_2(F_4TCNQ)(2,6\text{-lutidine})_2]$	**48**	BUKFIY	Pale yellow	1D
$[Cu^I_2(F_4TCNQ)(quinoline)_2]\cdot DMF$	**49**	BUKHAS	Pale yellow	1D
$[Cu^I_2(F_4TCNQ)(propionitrile)_2]$	**50**	QIXQAR	Colourless	1D
$[Cu^I_2(TCNQ)(2,2bipy)_2]\cdot 2H_2O$	**51**	BUKGEV	Red	1D
$[Cu^I_2(F_4TCNQ)(2,2bipy)_2]\cdot 2MeOH$	**52**	BUKJIC	Red	1D
$[Cu^I_2(TCNQ)(phen)_2]\cdot MeOH$	**53**	BUKGIZ	Red	1D
$[Cu^I_2(TCNQ)(Me_2bipy)]\cdot 2EtOH$	**54**	BUKGOF	Red	1D
$[Cu^I_2(TCNQ)(terpyridine)_2]$	**55**	BUKGAR	Red	1D
$[Cu^I_2(F_4TCNQ)(PPh_3)_3]$ (5)	**56**	BUKFOE	Pale yellow	1D
$[Cu^I_2(TCNQ)(Me_4en)_2]\cdot solvate$ (6)	**57**	BUKGUL	Colourless	1D
$[Cu^I_2(TCNQ)(Me_4en)_2]\cdot 2MeCN$ (6)	**58**	BUKHOG	Colourless	2D
$[Cu^I_2(F_4TCNQ)(PPh_3)_4]$ (5)	**59**	BUKHIA	Pale yellow	2D
$[Cu^I_2(TCNQ)(quinuclidine)_2]$	**60**	BUKHEW	Colourless	2D
$[Cu^I_2(TCNQ)(Me_2pyz)]$	**61**	BUKHUM	Red	2D
$[Cu^I_2(TCNQ)(apyz)_2]\cdot 5MeOH$	**62**	BUKJAU	Orange	3D
$(NEt_4)[Cu^I(F_4TCNQ)]$ (4a)	**63**	CUTMIP	Pale yellow	2D
$(MePPh_3)_2[Cd_2(TCNQ)_3]$	**64**	KOBFIR	Yellow	3D
$(MePPh_3)_2[Fe_2(TCNQ)_3]$	**65**	TONTIB	Yellow	3D
$(MePPh_3)_2[Co_2(TCNQ)_3]$	**66**	TONTOH	Red	3D
$(MePPh_3)_2[Ni_2(TCNQ)_3]$	**67**	TONTUN	Green	3D

Table 1 *(continued)*

Compound	Cp'd no.	CSD ref code	Colour	Type
$(MePPh_3)_2[Zn_2(TCNQ)_3]$[3]	**68**	TONVAV	Yellow	3D
$(PPh_3Me)_2[Zn_3(TCNQ)_3Br_2]$[3a]	**69**	CUTDEC	Yellow	2D
$[Mn(DMSO)_4(H_2O)_2][Mn_2(TCNQ)_3]$	**70**	FAKLIO	Pale green	3D
$[Cd(DMSO)_4(H_2O)_2][Mn_2(TCNQ)_3]$	**71**	FAKLOU	Pale yellow	3D
$[Zn(DMSO)_4(H_2O)_2][Mn_2(TCNQ)_3]$	**72**	FAKLUA	Pale yellow	3D
$[Mn(2,2bipy)_3][Mn_2(TCNQ)_3]$	**73**	FAKMAH	Red	3D
$(NMe_4)[Cu^I(F_4TCNQ)]\cdot H_2O$	**74**	KINMUR	Pale green	3D PtS
$(NMe_2Pr_2)[Cu^I(F_4TCNQ)]\cdot 3EtOH$	**75**	KINNAY	Pale yellow	3D PtS
$(NMe_2Bu_2)[Cu^I(F_4TCNQ)]\cdot 2EtOH$	**76**	KINNEC	Pale yellow	3D PtS
$(NEt_4)[Cu^I(F_4TCNQ)]\cdot DMSO$[4]	**77**	KINNIG	Pale yellow	3D PtS
$(PPh_4)[Cu^I(F_4TCNQ)]\cdot\frac{1}{2}DMF$	**78**	KINNOM	Dark green	3D PtS
$(MePPh_3)[Cu^I(F_4TCNQ)]\cdot DMF$	**79**	KINNUS	Yellow/green	3D PtS
$(NPr_4)[Cu^I(F_4TCNQ)]\cdot\frac{1}{2}MeCN$	**80**	DABMUR	Yellow	3D
$(NMe_4)[Cu^I(TCNQ)]$	**81**	YEVKAO	Colourless	3D PtS
$(NEt_4)[Cu^I(TCNQ)]$	**82**	CUTMAH	Colourless	3D PtS
$(NMe_2pent_2)[Cu^I(TCNQ)]$	**83**	CUSZIB	Colourless	3D PtS
$(Nspiro)[Cu^I(TCNQ)]\cdot 3DMSO$	**84**	YEVKES	Colourless	3D PtS
$(NPr_4)[Cu^I(TCNQ)]$	**85**	CUSYIA	Colourless	3D PtS
$(Mepyz)[Cu^I(TCNQ)]\cdot DMF$	**86**	CUSYUM	Black	3D PtS
$(Meiq)[Cu^I(TCNQ)]\cdot MeCN$	**87**	CUSZEX	Black	3D PtS
$(pnpyz)[Cu^I(F_4TCNQ)]$	**88**	CUXLEO	Red	3D PtS
$(dpx)_{1/2}[Cu^I(F_4TCNQ)]\cdot H_2O$	**89**	CUYDIL	Red	3D PtS
$(AsPh_4)[Cu^I(TCNQ)]\cdot$solvate	**90**	CUSZAT	Orange	3D PtS
$(PPh_4)[Cu^I(TCNQ)]\cdot MeCN$	**91**	CUSYOG	Red	3D PtS

(1) Products formed from the same reaction mixture in approximately equal proportions; (2a) is the minor product from the same reaction mixture as (2); (3a) is the minor product from the same reaction mixture as (3); (4a) is the minor product from the same reaction mixture as (4); (5) products formed from the same reaction mixture in approximately equal proportions; (6) products formed from the same reaction mixture in approximately equal proportions.

The compounds $[M^{II}(X_4TCNQ^{-II})(MeOH)_2]\cdot G$ (M = Zn, Mn or Cd; G = pyrazine, Me_2pyz, tmpyz, acridine, phenazine) (**11**–**17**) have slightly undulating 2D sheets that, apart from one exception (see below), adopt the type B geometry. The uncoordinated pyrazine-based molecules are able to form hydrogen bonds with the coordinated methanol ligands of neighbouring sheets to form 3D networks. The representative compound $[Zn(TCNQ)(MeOH)_2]\cdot$tmpyz (**14**) is shown in Fig. 3a. Compound **13**, which has the same composition as **14**, has the square grid, type A arrangement. The phenazine molecule in compound **16**, in addition to forming an H-bonded bridge between adjacent sheets, participates in a stacking interaction with the rings of the F_4TCNQ^{2-} ligands to either side (Fig. 3b). This facilitates a charge–transfer interaction that gives the crystals a red colour. In the structure of $[Mn(F_4TCNQ)(MeOH)_2]\cdot 2$acridine (**17**) each acridine molecule forms a hydrogen bond with one coordinated methanol and participates in aromatic stacking interactions with an F_4TCNQ^{2-} ligand and a symmetry-related acridine molecule which has a hydrogen bond to an adjacent sheet (Fig. 3c).

The combination of M^{II} centres (M = Mn, Zn, Co and Cd) and $TCNQ^{2-}$ with pyridine-based co-ligands (pyridine, 4-methylpyridine, quinoline and 4-phenylpyridine) (**18**–**24**) results in interdigitating 2D polymers that adopt the type B geometry.[78] The separation of co-ligands within a single sheet (~7.4 Å) corresponds to the short edge of a rectangle of metal centres (Fig. 2b), which appears ideal to promote interdigitation. Face-to-face contacts, half that of the short edge (~3.7 Å), occur between co-ligands of adjacent sheets. When pyridine (**18**) is substituted with 4-phenylpyridine (**21**), there is a marked increase in separation between sheets, resulting in larger solvent filled channels throughout the crystal structure as is apparent upon inspection of Fig. 4. The compound $[Zn(TCNQ)(nicotinamide)_2]$ (**25**) differs in that sheets are linked directly *via* complementary amide-amide double hydrogen bonds between nicotinamide ligands of neighbouring sheets. The resulting 3D H-bonded network is shown in Fig. 5. The orientation of the nicotinamide ligands results in intra-framework channels that are occupied by disordered solvent molecules.

The inclusion of chelating co-ligands such as 2,2bipy and 1,10-phenanthroline (phen) results in sheets with the 4,4-topology (**27**–**33**). In contrast to the gently undulating sheets formed when the co-ligands are *trans*, the occupation of the *cis* sites by the chelating ligands means that the sites available to the TCNQ ligand can only be occupied if the 4,4-networks adopt a highly corrugated structure.[79] An example of this corrugation which is apparent in [Cd(TCNQ)(phen)] (**31**) is presented in Fig. 6. The metal centres deviate significantly from the mean plane of the sheets, with the co-ligands sitting above or below the sheets. The compounds incorporating the $TCNQ^{2-}$ anion generally adopt the type A connectivity, whereas the type B connectivity is observed with the F_4TCNQ^{2-} analogues **29**, **30** and **33**.

The non-chelating ligands 4,4′-bipyridine (4,4bipy) and 1,2-bis(4-pyridyl)ethylene (bpe) are able to bridge metal

Table 2 Organic salts formed with the X_4TCNQ^{2-} anion

Compound	Cpd no.	CSD ref no.	Colour	Packing type	Est. charge[a]	Interaction
$[(enH)_2(en)]TCNQ$	**92**	MOYBUY	Colourless	Discrete	−2.00(6)	H-bonding
$(HNEt_3)_2TCNQ$	**93**	MOYCOT	Colourless	Discrete	−2.04(9)	H-bonding
$(TEAH)_2TCNQ$	**94**	MOYCUZ	Colourless	Discrete	−1.97(10)	H-bonding
$[(dabco{\cdot}H^+)_2(dabco)]TCNQ$	**95**	MOYBAE	Colourless	Discrete	−2.00(6)	Electrostatic
$(dbdab)F_4TCNQ$	**96**	BODZEB	Pale yellow	Pairs	−2.14(17) −2.29(17)	Electrostatic
$(Me_2dab)F_4TCNQ$	**97**	YEVJER	Colourless	Stacks	−2.04(10)	Electrostatic
$(Mev)F_4TCNQ$	**98**	BODZIF	Dark green	V	−1.93(6)	Face-to-face
(Mev)TCNQ	**99**	MOYCAF	Black	V	−2.01(9)	Face-to-face
$(Etv)F_4TCNQ$	**100**	DABMOL	Green	V	−1.90(7)	Face-to-face
(bv)TCNQ	**101**	MOYCEJ	Black	V	−1.94(6)	Face-to-face
$(dpmv)F_4TCNQ$	**102**	BODZOL	Black	V	−1.94(17)	Face-to-face
$(ddabx)F_4TCNQ$	**103**	BODZUR	Green	V	−2.14(11)	Face-to-face
(diquat)TCNQ	**104**	MOYBEI	Black	V	−1.86(6) −1.76(13)	Face-to-face
$(phv)F_4TCNQ$	**105**	YEVJIV	Black	V	−1.63(12)	Face-to-face
$(phv)F_4TCNQ{\cdot}2MeOH$	**106**	YEVJUH	Red	V	−1.95(6)	Face-to-face
$(dpbene)F_4TCNQ$	**107**	YEVHOZ	Red	V	−1.77(10)	Face-to-face
(dpbene)TCNQ	**108**	MOYBIM	Black	V	−1.95(5)	Face-to-face
$[Pt(2,2bipy)_2]TCNQ$	**109**	MOYCIN	Black	V	−1.76(6)	Face-to-face
(dpx)TCNQ	**110**	MOYBOS	Black	V	−1.94(5)	Edge-to-face
$(dpe)F_4TCNQ$	**111**	DABMIF	Red	V	−1.94(13)	Face-to-face
$(mnbp)_2F_4TCNQ$	**112**	BOFBAB	Black	VI	−1.86(7)	Face-to-face
$(dnbp)_2F_4TCNQ$	**113**	BODMEO	Black	VI	−2.05(8)	Face-to-face
$(Meiq)_2F_4TCNQ$	**114**	BODNAL	Black	VI	−1.97(6)	Face-to-face
$(mnbiq)_2F_4TCNQ$	**115**	BODYEA	Dark purple	VI	−2.02(7)	Face-to-face
$(dnbdab)F_4TCNQ$	**116**	BODYIE	Black	VI	−1.90(8)	Face-to-face
$(dcpx)F_4TCNQ$	**117**	DABXUC	Dark purple	VI	−1.79(13)	Face-to-face
$(phv)F_4TCNQ{\cdot}MeOH$	**118**	YEVJOB	Brown	VI	−1.96(13)	Face-to-face
$(pnbphp)F_4TCNQ$	**119**	BODYOK	Dark purple	VII	−1.88(5)	Edge-to-face
(pnbphp)TCNQ	**120**	BODYUQ	Dark purple	VII	−1.91(5)	Edge-to-face
$(p\text{-}spongeH)F_4TCNQ$	**121**	BODZAX	Pale yellow	VII	−1.99(8)	Edge-to-face
$[Zn(2,2bipy)_2(OAc)]TCNQ$	**122**	MOYDAG	Red	VII	−1.96(15)	Edge-to-face
$[Fe(phen)_3]F_4TCNQ$	**123**	YEVHUF	Red	VII	−2.02(8)	Edge-to-face
$(dbipx)F_4TCNQ$	**124**	DACCIW	Dark green	VII	−1.87(12)	Edge-to-face
$(dpx)F_4TCNQ$	**125**	BODMIS	Red	VIII	−2.09(6)	Segregated
$(dpicx)F_4TCNQ$	**126**	BODMOY	Red	VIII	−1.86(17)	Segregated
$(diqx)F_4TCNQ$	**127**	BODMUE	Dark red	VIII	−2.01(6)	Segregated

[a] Calculated from the Kistenmacher relationship.

centres in adjacent type A sheets (except for **42** which adopts the type B geometry) to form 3D coordination polymers of general composition $[M^{II}(TCNQ)(4,4bipy)]$ (M = Fe, Co, Cd, Zn and Mn) (**36–40**) and $[M^{II}(TCNQ)(bpe)]$ (M = Cd and Zn) (**41**, **42**).[78] The structure of $[Mn^{II}(TCNQ)(4,4bipy)]$ (**40**) is shown in Fig. 7. The sheets are slightly undulating and are linked together such that the 4,4bipy and bpe ligands act as 'pillars', resulting in large solvent filled intra-framework voids. The pale-yellow compound $[Zn^{II}(TCNQ)(4,4bipy)]{\cdot}$solvate was first reported by Kitagawa and co-workers, which was obtained *via* the disproportionation of $TCNQ^{\cdot-}$ in the presence of ascorbic acid.[69,80] Recently, Dunbar and co-workers reported that the compound $[Fe^{II}(TCNQ)(4,4bipy)]{\cdot}$solvate displayed solvent induced changes in magnetic behaviour at low temperature.[81]

The co-ligand 4,4′-bipyridine-1,1′-dioxide (Obip) bridges Zn(TCNQ) sheets in $[Zn(TCNQ)(Obip)_{1/2}(MeOH)]$ (**43**), as shown in Fig. 8. In contrast to the compounds discussed above, in which the 4,4bipy and bpe ligands are orientated perpendicular to the mean planes of the sheets, a bend at the oxygen atom of the Obip (N–O–Zn *ca.* 118°), enables a face-to-face interaction between the electron deficient aromatic rings of Obip with the electron rich $TCNQ^{2-}$ anions. The resulting charge transfer interaction leads to a deep red colour.

Neutral coordination polymers with Cu^I centres

As stated in the introduction, Cu^ITCNQ exists in two distinct phases each of which possesses interesting electrical properties. In each of these phases the Cu(I) centre is 4-coordinate and the $TCNQ^{\cdot-}$ ligand binds to four Cu(I) centres. When the dianionic form of TCNQ is employed, twice as many Cu(I) centres per TCNQ unit are required for electrical neutrality. Under these circumstances, in which there are potentially twice as many coordination sites, there is the opportunity for including co-ligands into the structure. This section describes a series of neutral $[Cu^I{}_2X_4TCNQ^{-II}]$ structures in which co-ligands also coordinate to the Cu(I) centres.

The combination of Cu^I and X_4TCNQ^{2-} with various co-ligands forms the series of neutral coordination polymers

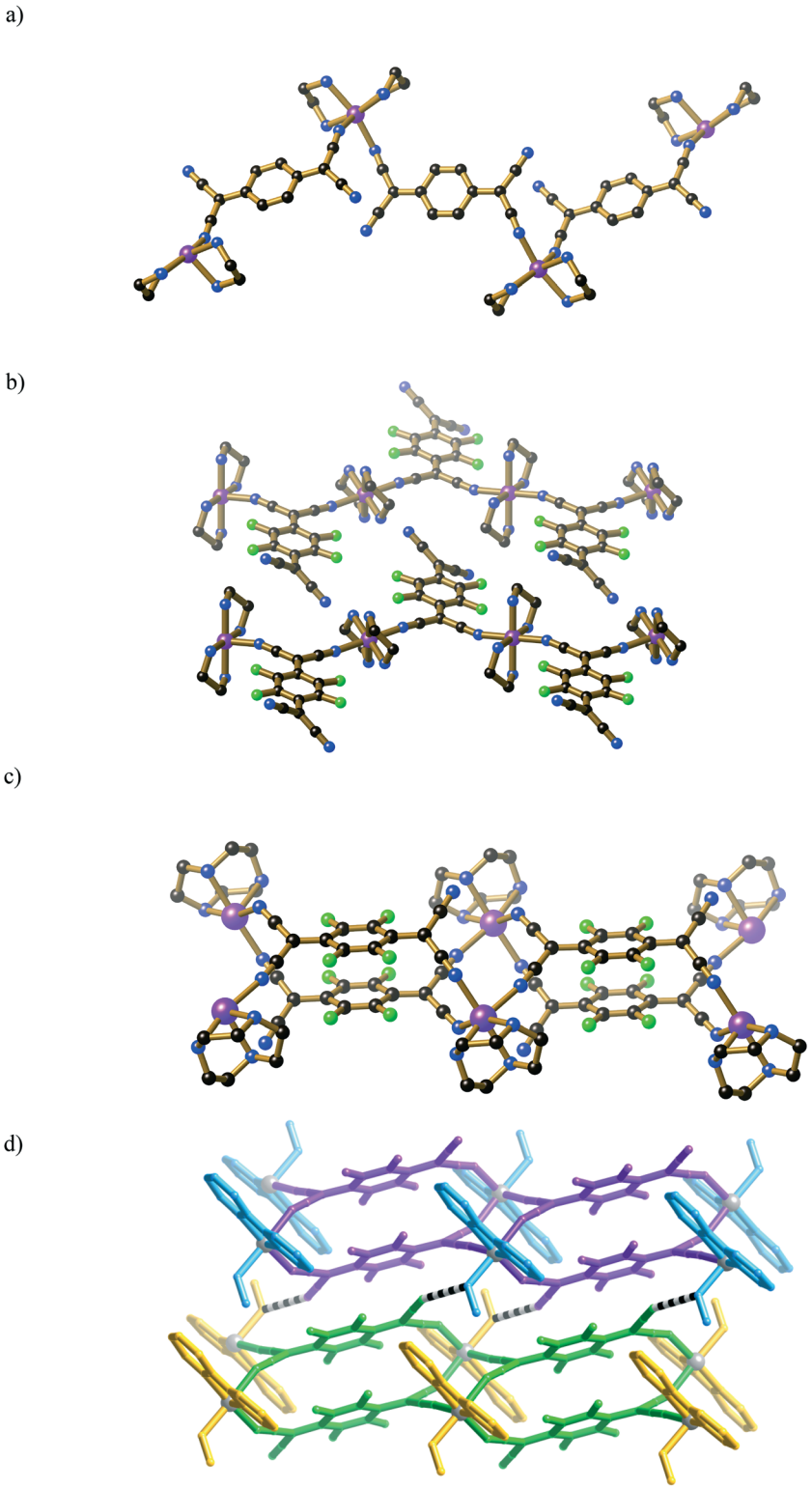

Fig. 1 1D coordination polymers in which divalent metal ions are linked by X_4TCNQ^{2-} ligands: a) a single chain of $[Mn(en)_2(TCNQ)]$ (**1**) b) interdigitating chains of $[Mn(en)_2(F_4TCNQ)]$ (**2**) c) a "double-layered" polymer of $[Cd(TACN)(F_4TCNQ)]$ (**4**) and d) a pair of "double-layered" polymers of $[Zn(F_4TCNQ)(2,2bipy)(MeOH)]$ (**6**) with hydrogen bonding between the chains indicated by striped connections.

with the general formula $[Cu^{I}_2(X_4TCNQ^{-II})(co\text{-}ligand)_y]$ (y = 1–4) (**44–62**).[82,83] The use of propionitrile co-ligands[82] or the planar co-ligands, 2-picoline, 2,6-lutidine, quinoline, isoquinoline and 4-phenylpyridine, results in the formation of interdigitating strip-like coordination polymers (**44–50**).[83] Within each strip, the C–X_4C_6–C axes of the X_4TCNQ^{2-} ligands are parallel, with the X_4TCNQ^{2-} ligands binding to four Cu^{I} centres, which lie at the corners of a rectangle.

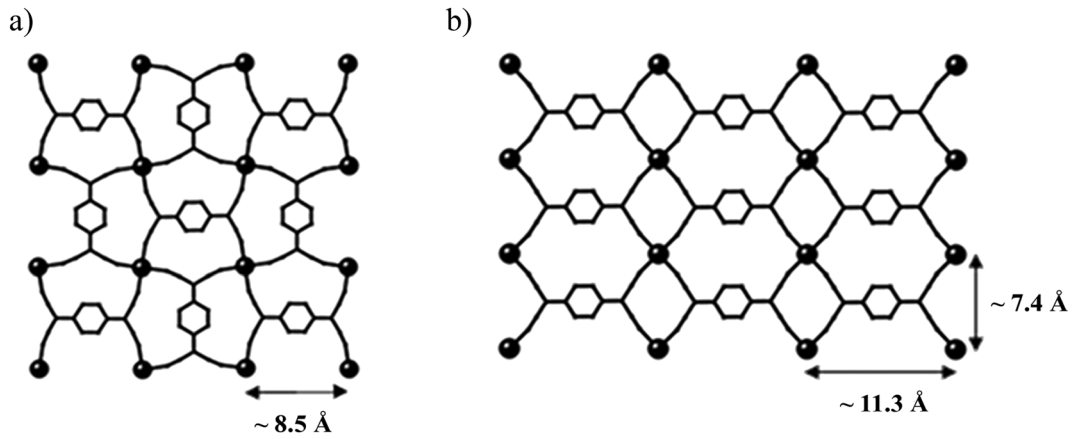

Fig. 2 The arrangement of metal centres; a) in a square grid (type A) in which the C–X_4C_6–C axes of the $TCNQ^{2-}$ ligands alternate in orientation, and b) in a rectangular grid (type B) with C–X_4C_6–C axes of the X_4TCNQ^{2-} units parallel.

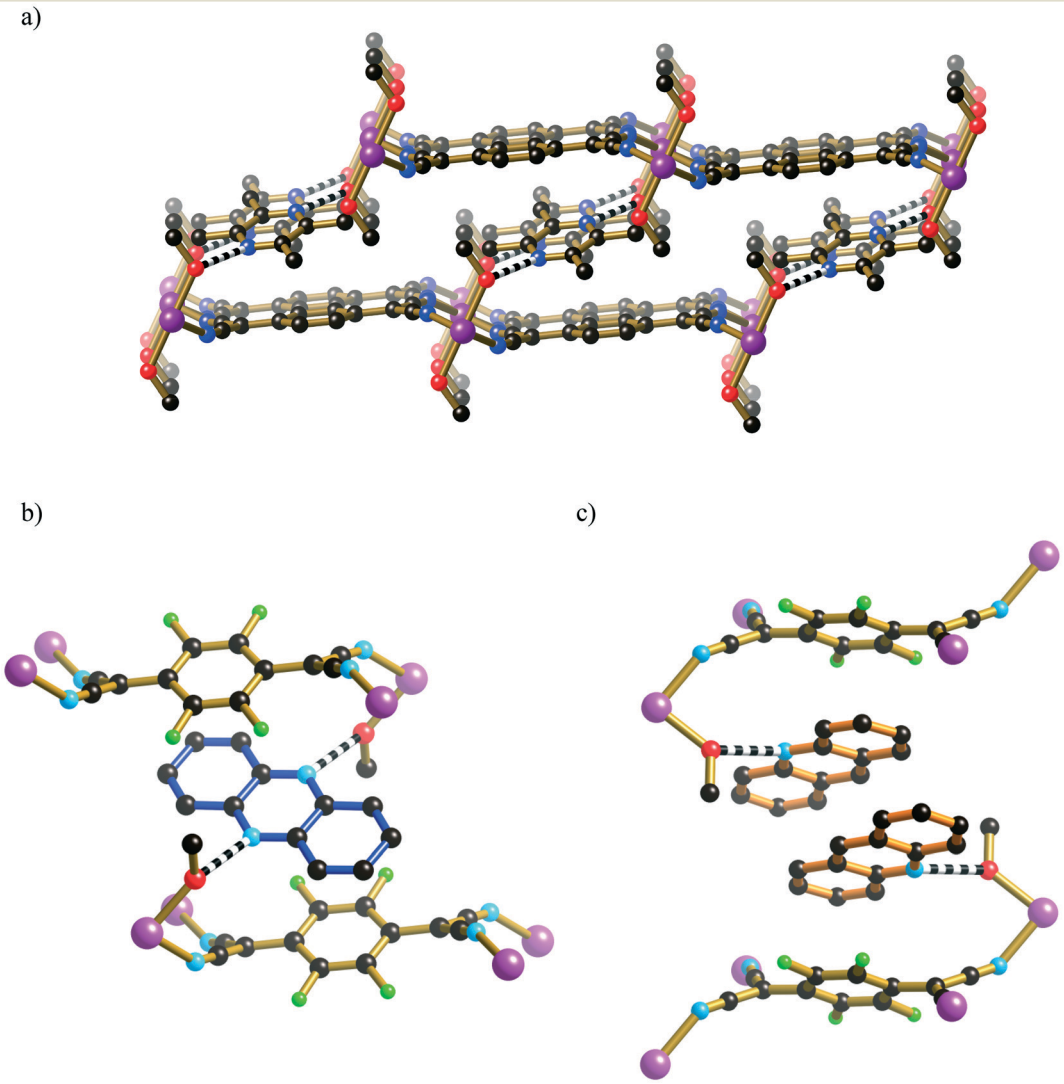

Fig. 3 a) The structure of [Zn(TCNQ)$(MeOH)_2$]·tmpyz (**14**) in which sheets are linked *via* H-bonding between coordinated MeOH ligands and tetramethylpyrazine units (H-bonds represented by striped connections). b) The structure of [Mn(F_4TCNQ)$(MeOH)_2$]·phenazine (**16**) showing the H-bonding and aromatic interactions of the phenazine molecule. c) The H-bonding and stacking in [Mn(F_4TCNQ)$(MeOH)_2$]·2acridine (**17**).

Each Cu^I centre has a trigonal planar geometry, coordinated by two X_4TCNQ^{2-} ligands and a terminal co-ligand. Close face-to-face interactions occur between co-ligands from neighbouring strips. The compound [Cu^I_2(TCNQ)(4-

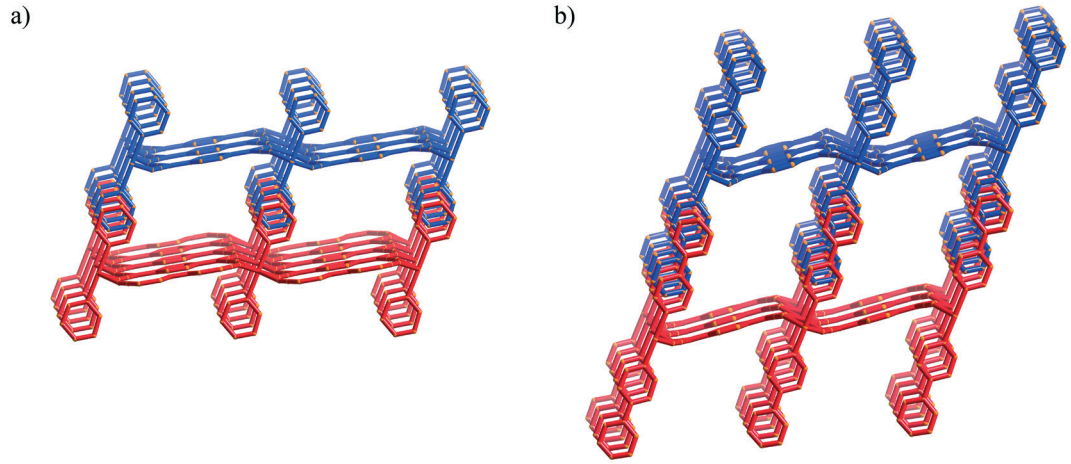

Fig. 4 Two interdigitating type B sheets in a) [Mn(TCNQ)(pyridine)$_2$] (**18**) and b) the increased sheet-sheet separation in [Zn(TCNQ)(phenylpyridine)$_2$] (**21**).

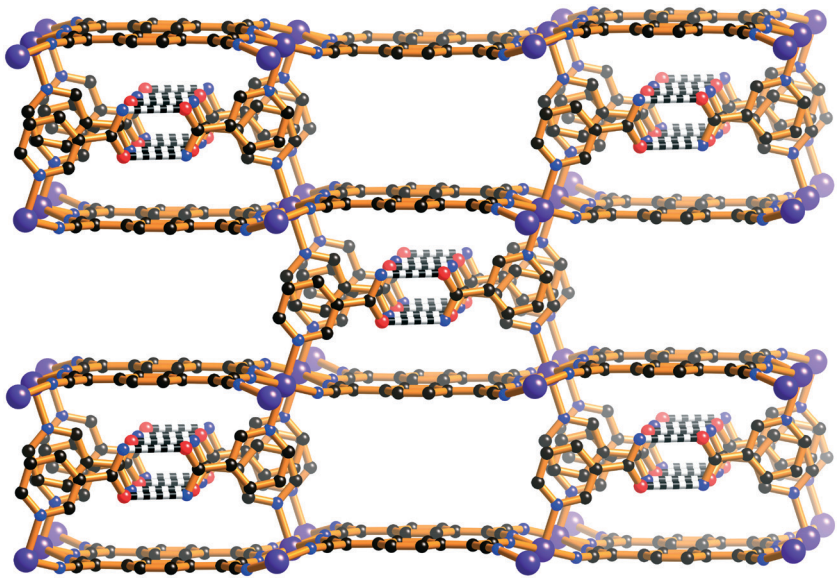

Fig. 5 The 3D hydrogen bonded network [Zn(TCNQ)(nicotinamide)$_2$] (**25**) (amide–amide H-bonds represented by striped connections).

phenylpyridine)$_2$] (**46**) which is representative of this class of compounds is presented in Fig. 9a. Similar interdigitating strips are formed with the chelating co-ligands 2,2bipy (**51**, **52**), phen (**53**) and 5,5′-dimethyl-2,2′-bipyridine (Me_2bipy) (**54**), in which the Cu^I centres adopt a tetrahedral geometry, in addition to terpyridine (**55**) in which the Cu^I centre is 5-coordinate. The compound [$Cu^I_2(F_4TCNQ)(PPh_3)_3$] (**56**) also forms a strip, with a combination of Cu^I centres, in which trigonal Cu^I centres are each bound to a single PPh_3 ligand and tetrahedral Cu^I centres, are each bound to a pair of PPh_3 ligands.

The chelating ligand *N*,*N*,*N*′*N*′-tetramethylethlenediamine (Me_4en) when combined with Cu^I and $TCNQ^{2-}$ generates slightly undulating strips of composition [Cu^I_2(TCNQ)(Me_4-en)$_2$]·solvate (**57**). In contrast to the structures discussed above, in which the co-ligands are ostensibly planar, the Me_4en ligands are too bulky to allow interdigitation. Within the same reaction mixture which produced **57**, a 2D coordination polymer (**58**), similar in composition, is also formed. The sheet structure is topologically identical to that observed in the compounds [$Cu^I_2(F_4TCNQ)(PPh_3)_4$] (**59**) and [Cu^I_2(TCNQ)(quinuclidine)$_4$] (**60**), which is represented in Fig. 9b.

There are two examples to date in which Cu^I_2(TCNQ)-type structures include bridging co-ligands. The compound [Cu^I_2(TCNQ)(Me_2pyz)] (**61**) comprises near planar 2D networks. Although **61** may be considered to possess the same Cu^I_2(TCNQ) topology as compounds **58–60**, the overall connectivity arising from the participation of bridging 2,5-dimethylpyrazine (Me_2pyz) ligands yields the 2D network depicted in Fig. 10a in which the Cu(I) centres are trigonal. The compound [Cu^I_2(TCNQ)(apyz)$_2$] (**62**), contains [Cu^I_2TCNQ] strips which are linked to neighbouring strips by disordered 2-aminopyrazine (apyz) bridges, to form the 3D coordination polymer shown in Fig. 10b which possesses channels with approximately hexagonal cross-section.

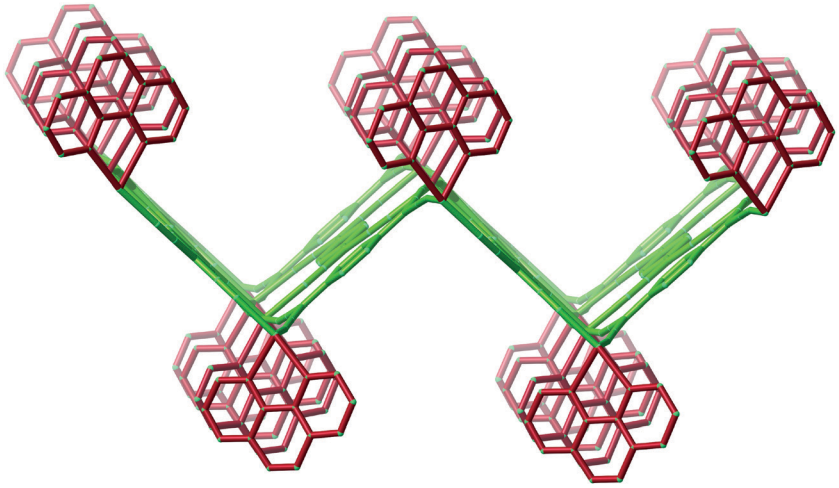

Fig. 6 The highly corrugated sheet structure of [Cd(TCNQ)(phen)] (**31**).

2. Anionic coordination polymers

This section describes coordination polymers that carry a net negative charge. As with the previous section this is divided into two parts, 1) structures in which the X_4TCNQ^{2-} ligands are linked by divalent metal ions and 2) structures which contain Cu(I) centres.

Anionic networks of general formula $[M^{II}_2(X_4TCNQ^{-II})_3]^{2-}$

A series of $TCNQ^{2-}$ derived anionic coordination polymers, of general formula $[M^{II}_2(TCNQ^{-II})_3]^{2-}$, have been reported in which both the choice of counter-cation and metal centre has had a significant impact on the resulting network topologies.[75,84,85] The reaction of $Cd(NO_3)_2$, $TCNQH_2$, LiOAc and $MePPh_3Br$ leads to the formation of a network material with formula, $(MePPh_3)_2[Cd^{II}_2(TCNQ)_3]$ (**64**).[75] The compound crystallises in the space group $R\bar{3}$. The 3D network comprises slightly distorted octahedral Cd^{II} centres, which adopt a pseudo-primitive-cubic arrangement (Fig. 11). The $TCNQ^{2-}$ ligands bind to four Cd^{II} centres, with each octahedral Cd^{II} centre coordinated by six planar $TCNQ^{2-}$ anions. For simplicity, the framework can be divided into "octants", as illustrated in Fig. 11, in which the $MePPh_3^+$ counter-cations reside. Within each octant, only half of the six faces are occupied by $TCNQ^{2-}$ ligands.

The family of isostructural compounds $(MePPh_3)_2[M^{II}_2(TCNQ)_3]$ (M = Zn, Ni, Co, Fe) (**65–68**),[84] formed under very similar reaction conditions to the Cd derivative, form 3D coordination polymers with a markedly different network topology (Fig. 12). In contrast to the planar $TCNQ^{2-}$ ligands present in the $[M^{II}_2(TCNQ)_3]^{2-}$ framework, the NC–C–CN moieties are rotated out of the plane of the central aromatic ring. Pairs of $MePPh_3$ cations, which interact *via* a hexaphenyl embrace, occupy the intra-framework voids. Magnetic studies reveal long-range magnetic ordering within the networks.

The compounds $(M^{II}(DMSO)_4(H_2O)_2)[M^{II}_2(TCNQ)_3]$ (M = Mn, Zn, Cd) (**70–72**)[85] consist of 3D honeycomb-type networks, in which disordered metal complexes serve as counter-cations. The $[Cd_2(TCNQ)_3]^{2-}$ (**71**) framework is shown in Fig. 13a. Large parallel hexagonal channels, *ca.* 15 Å in diameter, are present throughout the structure, with the network atoms occupying less than half of the crystal volume. The $TCNQ^{2-}$ units are oriented such that the C–H_4C_6–C axes of the $TCNQ^{2-}$ units are inclined relative to the channel walls (Fig. 13b). The $[Mn_2(TCNQ)_3]^{2-}$ network, in which the metal complex $[Mn(2,2bipy)_3]^{2+}$ serves as the counter-cation, is topologically identical, however the orientation of the $TCNQ^{2-}$ anions is noticeably different. In the case of $(Mn^{II}(2,2bipy)_3)[Mn^{II}_2(TCNQ)_3]$ (**73**), the C–H_4C_6–C axes are oriented parallel to the channel walls, with the $TCNQ^{2-}$ anions located above and below the mean plane of the walls in an alternating fashion (Fig. 13c). Crystals of $(Mn^{II}(2,2bipy)_3)[Mn^{II}_2(TCNQ)_3]$ are a deep red, suggestive of charge transfer interactions between the cations and the network.

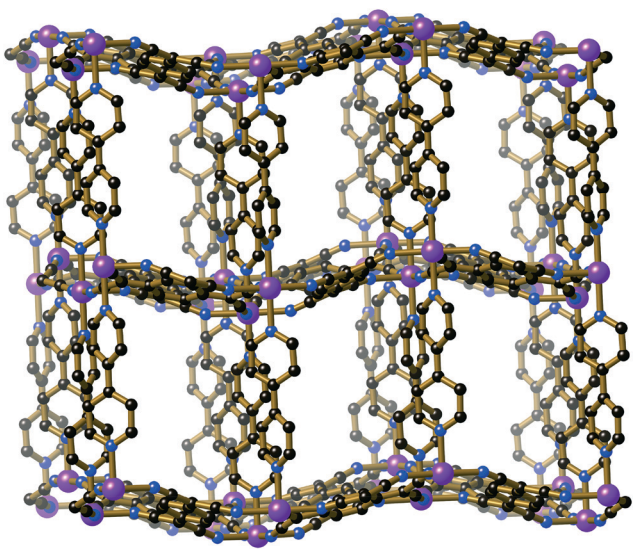

Fig. 7 The 3D pillared structure of $[Mn^{II}(TCNQ)(4,4bipy)]$ (**40**). Disordered solvent molecules occupy the large intra-framework voids.

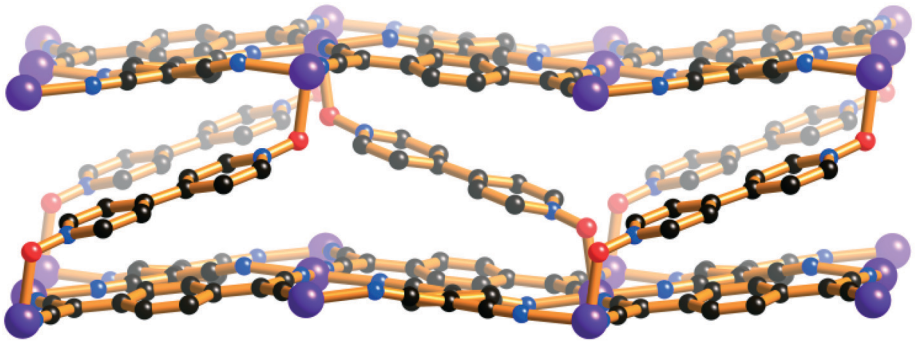

Fig. 8 The structure of [Zn(TCNQ)(Obip)$_{1/2}$(MeOH)] (**43**). The Obip ligands are inclined with respect to the sheets to form close charge transfer interactions with the $TCNQ^{2-}$ ligands. For clarity, the coordinated MeOH ligands have been omitted.

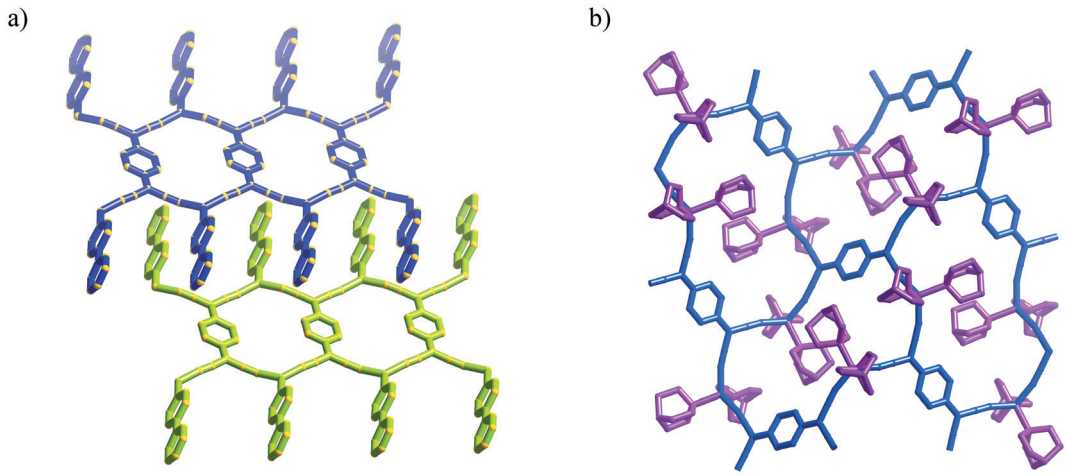

Fig. 9 a) Two interdigitating strips in [Cu^{I}_2(TCNQ)(4-phenylpyridine)$_2$] (**46**). b) The 2D sheet structure of [Cu^{I}_2(TCNQ)(quinuclidine)$_4$] (**60**).

Anionic networks of general formula $[Cu^{I}(X_4TCNQ^{-II})]^-$

One of the most important networks targeted in the generation of coordination polymers is the PtS net, which consists of 4-connecting tetrahedral centres and 4-connecting square planar centres in equal proportions, as depicted in Fig. 14. In its most symmetrical form the network is tetragonal and possesses channels of square and hexagonal cross-section which run perpendicular to the *c*-axis. As previously discussed, the electrically neutral coordination polymers $[M^{I}(TCNQ^{\bullet-})]$ (M = Ag, Cu) adopt the PtS topology, with both $[Ag^{I}(TCNQ^{\bullet-})]$ and phase II of $[Cu^{I}(TCNQ^{\bullet-})]$ each existing as interpenetrating neutral networks. With the general tendency of Cu^{I} to adopt a tetrahedral geometry, combined with the ability of X_4TCNQ^{2-} anions to bind to four metal centres in a planar arrangement, it was anticipated that an anionic coordination polymer of composition $[Cu^{I}(X_4TCNQ^{-II})]^-$ may also adopt the PtS topology. The negative charge on the network resulting from the incorporation of a dianionic ligand in place of the radical monoanionic ligand requires the incorporation of an appropriately sized counter-cation which would occupy the intraframework voids. The presence of a cation reduces the space available for a second network, thus preventing interpenetration. The following discussion relates to structures composed of an anionic $[Cu^{I}(X_4TCNQ)]^-$ network with various cations located in the framework channels.

A family of F_4TCNQ^{2-} derived compounds with the general formula $[Cu^{I}(F_4TCNQ)]^-$ (**74–79**) comprising networks with the PtS topology was reported in 2013.[86] Similar compounds have been subsequently synthesised (**81–91**). Compound **80** adopts a related structure with a complex topology.

The colourless compound $(NMe_4)[Cu^{I}(TCNQ)]$ (Fig. 15) (**81**) adopts the PtS-type network in which tetrahedral Cu^{I} centres are bound to four $TCNQ^{2-}$ ligands and each planar ligand is coordinated to four Cu^{I} centres at the corners of a rectangle. The C–H_4C_6–C axes of the $TCNQ^{2-}$ anions are oriented parallel to the *c*-axis, with ligands linked along this direction alternating in orientation by 90°. The elongated hexagonal channels are occupied by NMe_4^+ counter-cations. The "floor" and "ceiling" of the channels are separated by a distance corresponding to the short edge of a rectangular 'Cu^{I}_4TCNQ' unit (~7.5 Å). The compound is highly symmetrical, crystallising in the tetragonal space group $P4_2/mmc$, as does PtS itself. The compounds (cation)$[Cu^{I}(F_4TCNQ)]$ (cation = NMe_4^+, $NMe_2Pr_2^+$ and $NMe_2Bu_2^+$) (**74–76**) have very similar tetragonal networks, however, unlike the $TCNQ^{2-}$ anions in $(NMe_4)[Cu^{I}(TCNQ)]$, rotational disorder of the 'F_4C_6' cores with respect to CN–C–CN moieties are observed due to steric factors associated with the larger fluorine atoms.

The presence of the counter-cations NEt_4^+, $NMe_2Pent_2^+$ and $Nspiro^+$ **77**, **82–84** results in a lowering of network symmetry,

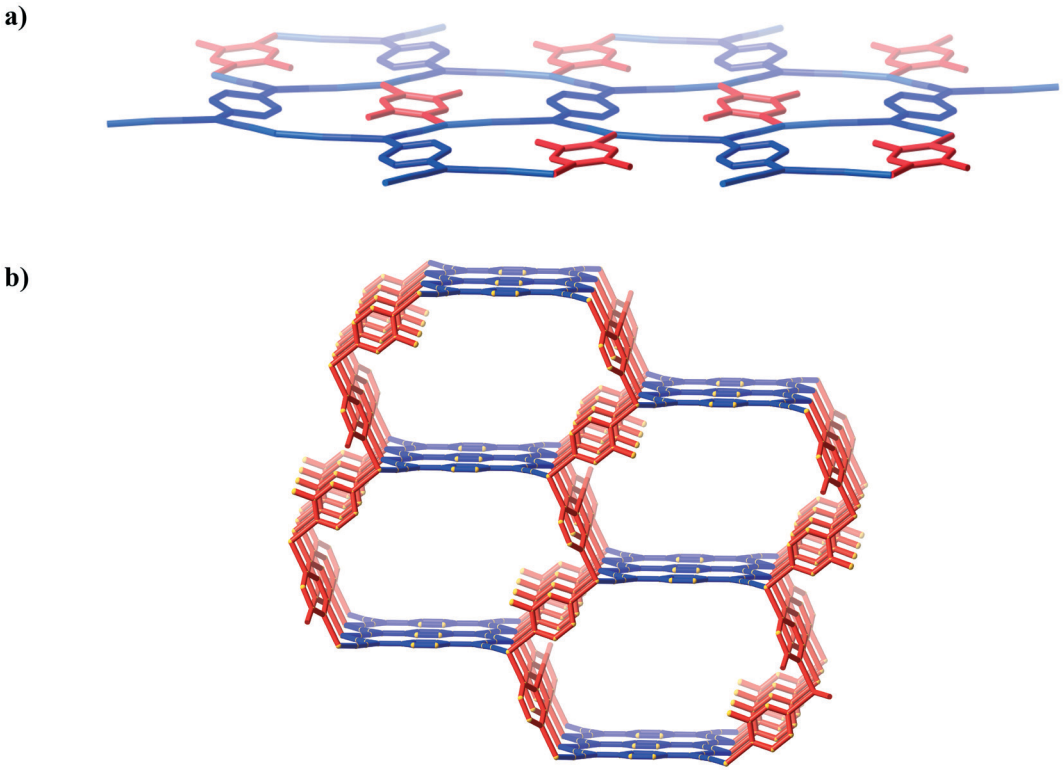

Fig. 10 a) The 2D sheet structure of $[Cu^{I}_2(TCNQ)(Me_2pyz)_2]$ (**61**) ($TCNQ^{2-}$ represented in blue; Me_2pyz represented in red). b) The 3D coordination polymer $[Cu^{I}_2(TCNQ)(2\text{-aminopyrazine})_2]$ (**62**); for clarity, only one orientation of the disordered 2-aminopyrazine ligands is shown ($TCNQ^{2-}$ represented in blue; 2-aminopyrazine represented in red).

with the Cu^{I} centres adopting a distorted tetrahedral geometry. A reduction of network symmetry is also apparent in $(Mepyz)[Cu^{I}(TCNQ)]$ (**86**) (Fig. 16). The concertina-like collapse of the network, most evident when viewed down the pseudo-tetragonal axis (Fig. 16b), presumably occurs to maximise the $TCNQ^{2-}$-cation interactions (closest contact *ca.* 3.1 Å). The hexagonal channels within the network are occupied by the cations

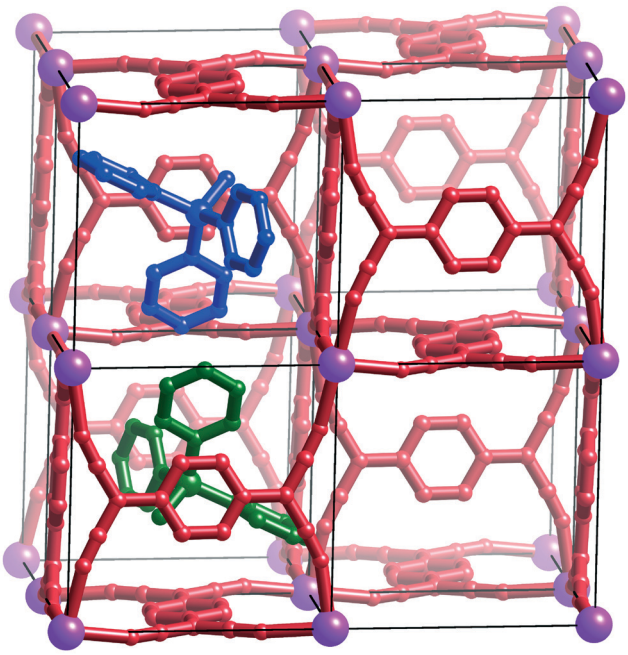

Fig. 11 A representation of $(MePPh_3)_2[Cd^{II}_2(TCNQ)_3]$ (**64**) illustrating the pseudo-cubic arrangement of Cd centres. For clarity, only two $MePPh_3^+$ cations, which occupy "octants" within the framework are shown.

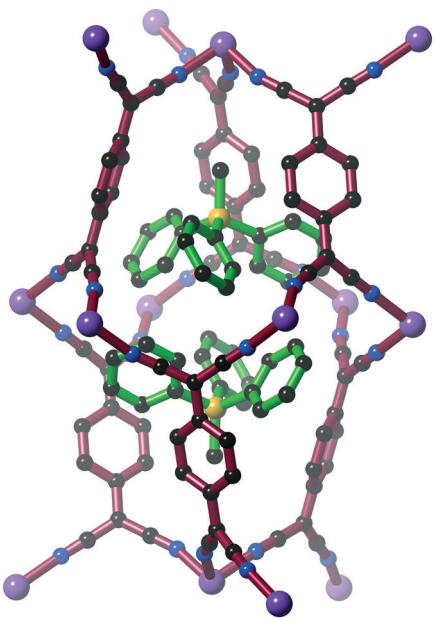

Fig. 12 The structure of $(MePPh_3)_2[M^{II}_2(TCNQ)_3]$ (M^{II} = Zn, Ni, Co, Fe) (**65–68**) in which there is a significant twist in the $TCNQ^{2-}$ ligands. Pairs of $MePPh_3^+$ cations (green) occupy the intra-framework cavities.

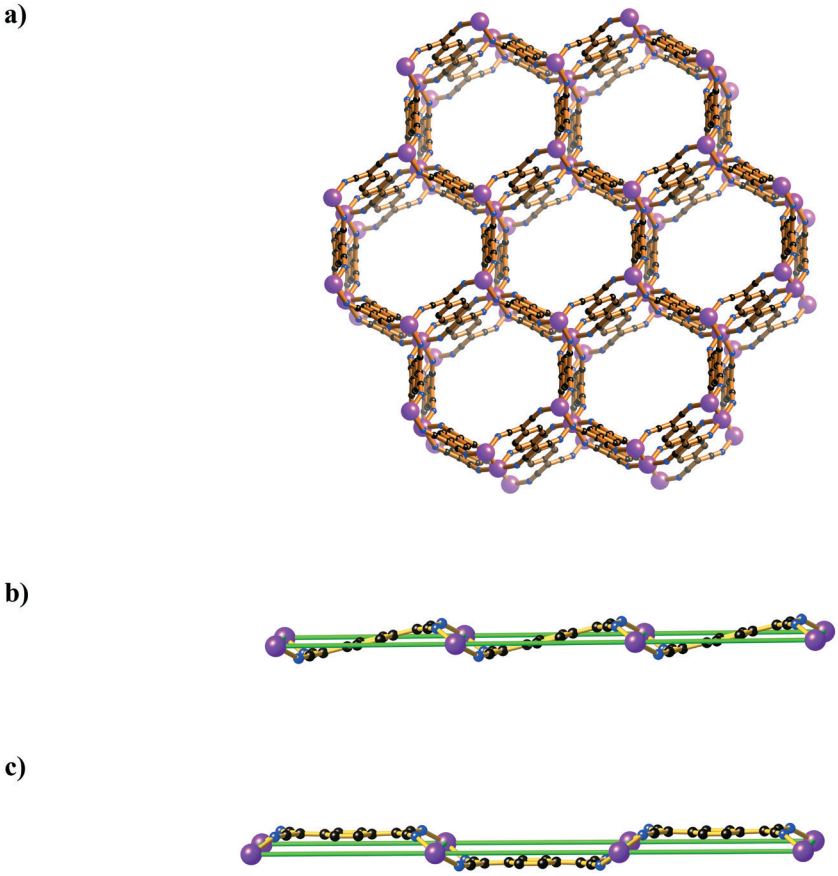

Fig. 13 a) The hexagonal $[Cd_2(TCNQ)_3]^{2-}$ network in $(Cd(DMSO)_4(H_2O)_2)[Cd_2(TCNQ)_3]$ (**71**). b) and c) The orientation of the coordinated $TCNQ^{2-}$ ligands with respect to the mean plane of the metal centres within $(M^{II}(DMSO)_4(H_2O)_2)[M^{II}{}_2(TCNQ)_3]$ (M^{II} = Mn, Zn, Cd) (**70**–**72**) and $(Mn^{II}(2,2bipy)_3)[Mn^{II}{}_2(TCNQ)_3]$ (**73**) respectively.

and DMF solvent molecules (Fig. 16c). The compound is almost black, indicative of charge–transfer between the cations and the electron-rich $TCNQ^{2-}$ anions. Comparable networks with very close donor–acceptor contacts are observed in compounds $(Meiq)[Cu^I(TCNQ)]$ (**87**), $(pnpyz)[Cu^I(F_4TCNQ)]$ (**88**), and $(dpx)_2[Cu^I(F_4TCNQ)]$ (**89**) which are also darkly coloured.

The compounds $(AsPh_4)[Cu^I(TCNQ)]$ (**90**), $(PPh_4)[Cu^I(F_4TCNQ)]$ (**78**), $(PPh_4)[Cu^I(TCNQ)]$ (**91**) and $(MePPh_3)[Cu^I(F_4TCNQ)]$ (**79**) adopt the PtS-type topology, however significant differences exist between these structures and those described above. The C–X_4C_6–C axes of the X_4TCNQ^{2-} ligands are oriented differently (see Fig. 17), with the separation of the $TCNQ^{2-}$ units occupying the floor and ceiling of the channels corresponding to the long axis of a "$Cu^I{}_4TCNQ$" rectangle (~11.6 Å). The intra-framework channels, which now adopt an approximately rectangular cross-section, are large enough to accommodate the bulkier cations. The structure of $(AsPh_4)[Cu^I(TCNQ)]$ is shown in Fig. 17. In each case, a phenyl group of the cation is 'sandwiched' between two X_4TCNQ^{2-} ligands, resulting in the formation of infinite X_4TCNQ^{2-}/H_4C_6 stacks, to give highly coloured compounds.

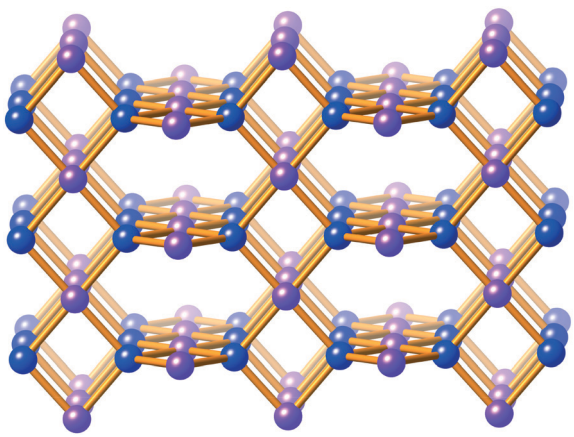

Fig. 14 The platinum sulphide network (Pt, purple; S, blue).

3. Organic charge transfer salts: cation – X_4TCNQ^{2-} complexes

A wide range of "organic complexes" involving the $X_4TCNQ^{\bullet-}$ radical species have been reported to date.[3,7] Such complexes are intensely coloured and almost always involve close π–π interactions between $TCNQ^{\bullet-}$ units that often are present within the crystal structure as closely associating pairs. In contrast, complexes involving the dianionic species (Table 2), have a

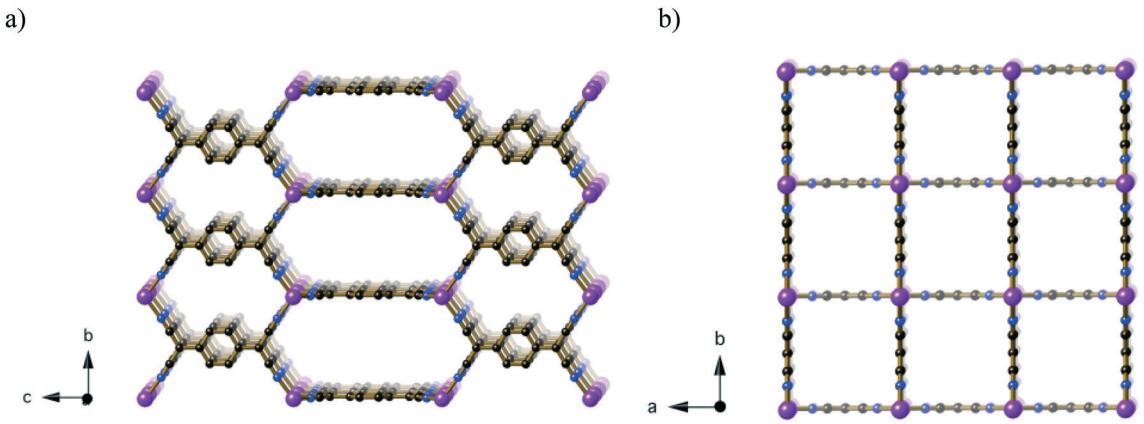

Fig. 15 The high symmetry $[Cu^{I}(TCNQ)]^{-}$ network in $(NMe_4)[Cu^{I}(TCNQ)]$ (**81**) viewed a) down the *a* axis and b) along the unique tetragonal axis. The NMe_4^{+} cations have been omitted.

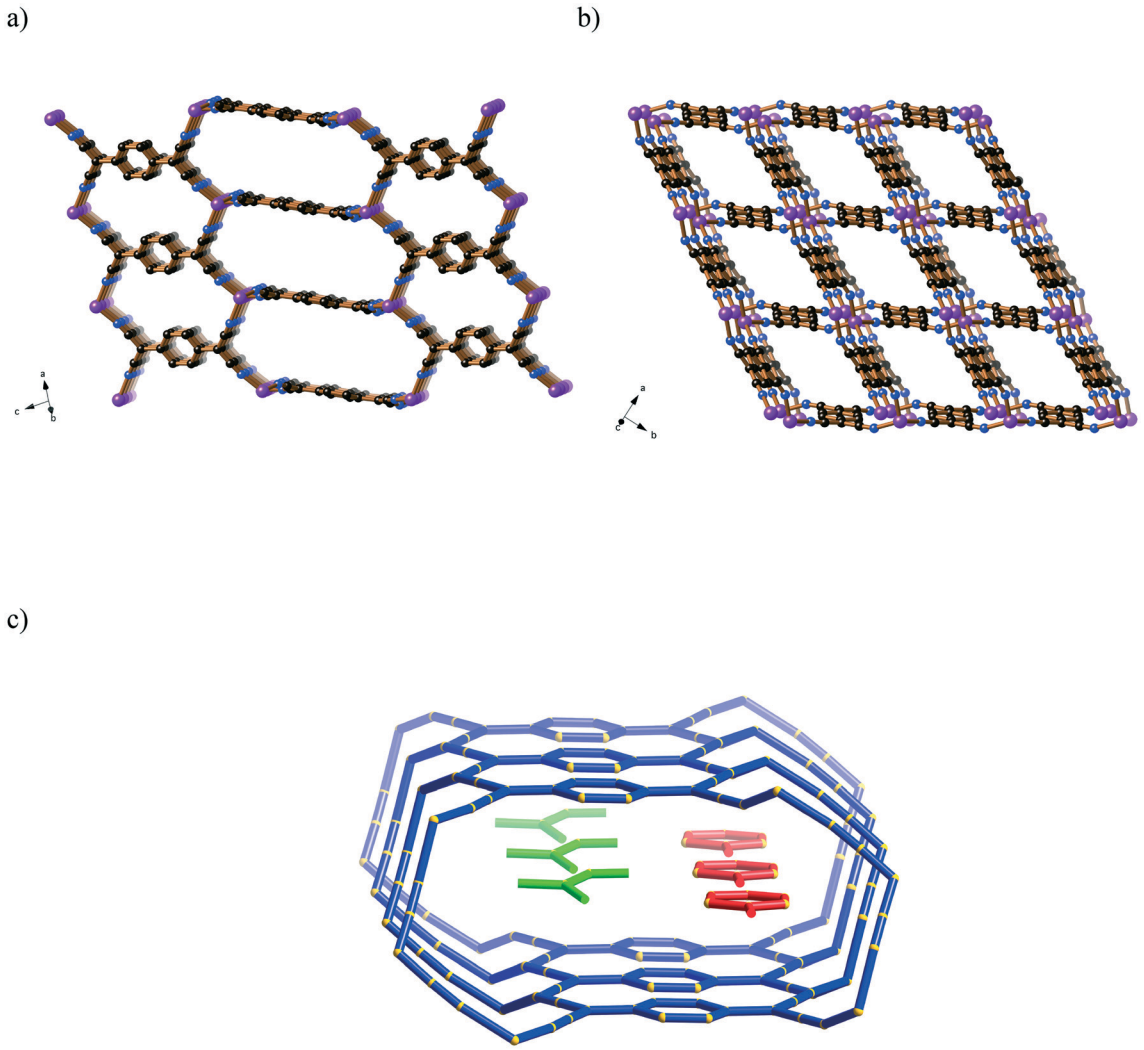

Fig. 16 The distorted $[Cu^{I}(TCNQ)]^{-}$ network in $(Mepyz)[Cu^{I}(TCNQ)]$ (**86**) viewed a) slightly off the *b* axis and b) slightly off the pseudo-tetragonal axis. The Me-pyrazinium cations have been omitted. c) View along a single hexagonal channel in $(Mepyz)[Cu^{I}(TCNQ)]$ occupied by $Mepyz^{+}$ cations (red) and DMF molecules (green).

propensity to exist as discrete anions (with a few exceptions which are discussed below) (**92–127**).[87,88] As previously discussed, the neutral forms of X_4TCNQ act as acceptors in charge transfer complexes, whereas the radical monoanion,

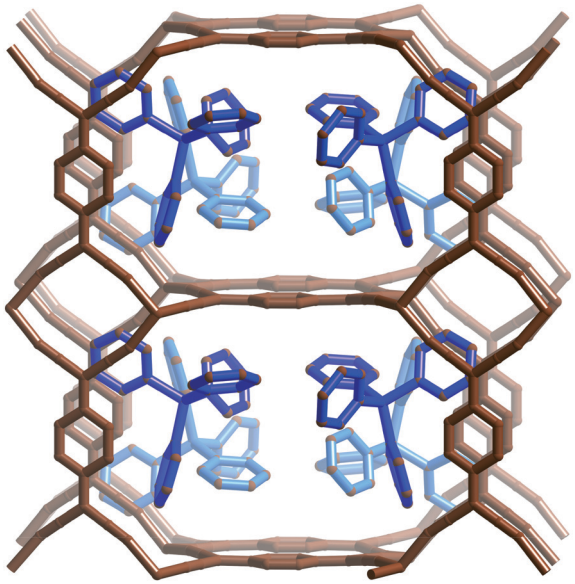

Fig. 17 The structure of $(AsPh_4)[Cu^{I}(TCNQ)]$ (**79**). The intra-framework voids are large enough to accommodate the bulky $AsPh_4^+$ cations (represented in blue).

$X_4TCNQ^{\bullet-}$ has the potential to act as both a donor and acceptor. The electron-rich dianionic species, X_4TCNQ^{2-} can serve only as a donor. Compounds involving the dianion with an assortment of cations range from colourless to black, indicative of varying degrees of charge transfer between X_4TCNQ^{2-} donors and acceptor cations. The cation–anion Coulombic interaction between cations and X_4TCNQ^{2-} anions is commonly supported by directional secondary interactions including hydrogen bonding, as well as edge-to-face and face-to-face van der Waals interactions involving planar units. The compounds described in this section represent solid-state examples of cases in which the X_4TCNQ^{2-} dianion is crystallised with appropriate cations. The cations reported here are depicted in Scheme 1.

The combination of the spin-paired $TCNQ^{2-}$ dianion with "innocent" cations, which are inherently unable to act as π-acceptors, largely results in the formation of colourless compounds. The complexes $[(enH^+)_2(en)]TCNQ$, $(Et_3NH^+)_2TCNQ$ and $(TEAH)_2TCNQ$ (**92–94**) are comprised of $TCNQ^{2-}$ units hydrogen bonded, *via* the nitrile groups, to protonated amines. The structure of $(Et_3NH^+)_2TCNQ$ (**93**) is shown in Fig. 18a. The colourless compound $[(dabco{\cdot}H^+)_2(dabco)]TCNQ$ (**95**), shown in Fig. 18b, is composed of strips of parallel $TCNQ^{2-}$ anions that interact electrostatically with the internally hydrogen bonded ($dabcoH^+$–dabco–$^+$Hdabco) trimers. The very pale yellow compound dbdab–F_4TCNQ (**96**) is unusual in that it contains discrete pairs of F_4TCNQ^{2-} dianions, which interact electrostatically with the surrounding cations (Fig. 18c).

The crystal packing arrangements of complexes that involve either edge-to-face or face-to-face π- interactions can be broadly divided into four categories (**V–VIII**), shown schematically in Fig. 19. The category **V** crystal packing arrangement, observed in compounds **98–111**, consists of infinite "stacks" of alternating dications and X_4TCNQ^{2-} dianions. A representative example is the compound $(Mev)F_4TCNQ$ (**98**), shown in Fig. 20a. Within a column, Mev^{2+} cations and F_4TCNQ^{2-} units are co-planar and associate through close face-to-face π-interactions. The orientation of the C–F_4C_6–C axes of the dianions is offset slightly from the long axes of the cations. Subtle variations are observed in other type **V** packing compounds. The compound (bv)TCNQ (**101**), comprises co-planar cations and anions associating in a face-to-face manner, however, the mean planes of both entities are significantly tilted with respect to the stacking direction. The steric imposition of the phenyl groups in $(dpmv)F_4TCNQ$ (**102**) results in a perpendicular orientation of the C–F_4C_6–C axis of the F_4TCNQ^{2-} anion and the long axis of the cation. The compound (dpx)TCNQ (**110**) is the only compound with the type **V** packing to date in which edge-to-face interactions between cations and anions are present (Fig. 20b). It is notable that the majority of the type **V** packing family of compounds are black, consistent with strong charge–transfer interactions.

Type **VI** packing consists of infinite stacks in which discrete F_4TCNQ^{2-} anions are separated by pairs of cations, with face-to-face interactions between the donors and acceptors (**112–118**). The compound $(Meiq)_2F_4TCNQ$ (**114**) is shown in Fig. 21a. The cations and anions are co-planar, with the mono-cations making close contact on both sides of the F_4TCNQ^{2-} anion. Similar structures are observed for compounds $(dnbp)_2F_4TCNQ$ (**113**) and $(mnbiq)_2F_4TCNQ$ (**115**), however, interesting variations in donor–acceptor interactions are observed. The structurally similar cations each possess two potential components able to associate with the F_4TCNQ^{2-} anion, with the isoquinolinium moiety of $mnbiq^+$ and the di-nitrobenzyl component of $dnbp^+$ preferentially participating in close face-to-face contacts with the anion. The dication containing compound $(dnbdab)F_4TCNQ$ (**116**) comprises linked stacks in which the singly charged moieties associate with the F_4TCNQ^{2-} anions in neighbouring stacks, as illustrated in Fig. 21b.

Type **VII** packing is very similar to the type **VI** packing, however the anions and the cations associate *via* edge-to-face interactions (**119–124**). The compound $(p\text{-}sponge{\cdot}H^+)_2F_4TCNQ$ (**121**) consists of stacks in which pairs of cations associate with each other in a face-to-face manner and edge-to-face with the anions, as shown in Fig. 22a. A similar packing arrangement is observed within the compound $(dbipx)F_4TCNQ$ (**124**), wherein the stacks are linked by the dications, with bipyridylium units from separate dications forming edge-to-face contacts with the anions (Fig. 22b).

The type **VIII** packing arrangement comprises discrete stacks of F_4TCNQ^{2-} dianions and xylene-based dications (**125–127**) – an unexpected arrangement, given that it would be anticipated that molecules possessing the same higher charge of 2+ or 2−, would result in significant Coulombic repulsions. The positive charges on the cations, however, are located on the pyridyl rings and therefore well separated, minimising the repulsion. The compound $(dpx)F_4TCNQ$ (**125**), which has a markedly different packing arrangement

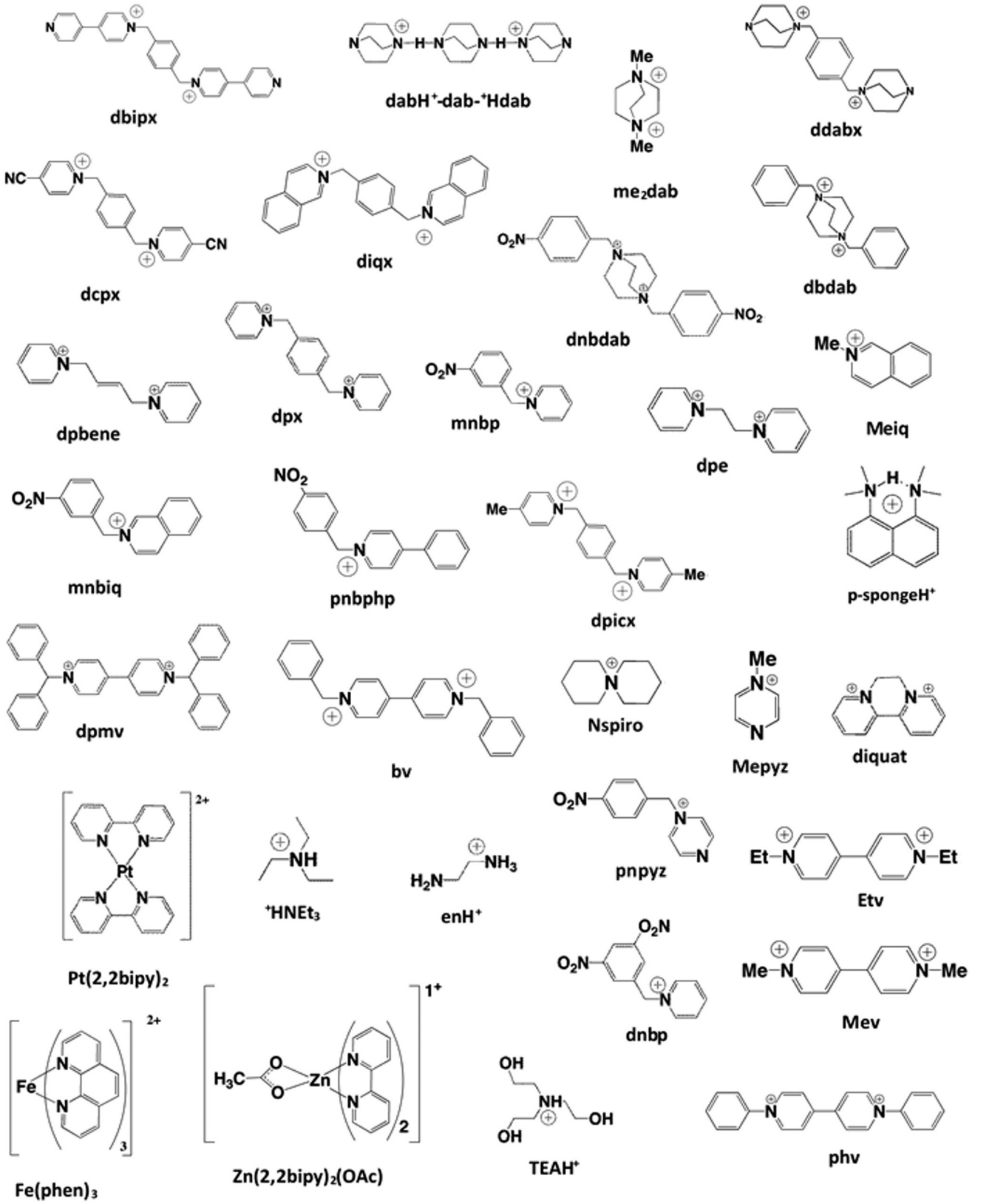

Scheme 1

to the $TCNQ^{2-}$ analogue (**110**), is shown in Fig. 23. The C–F_4C_6–C axes of the F_4TCNQ^{2-} anions are orientated in an alternating fashion along an anionic column, with similar alternation present within a column of cations.

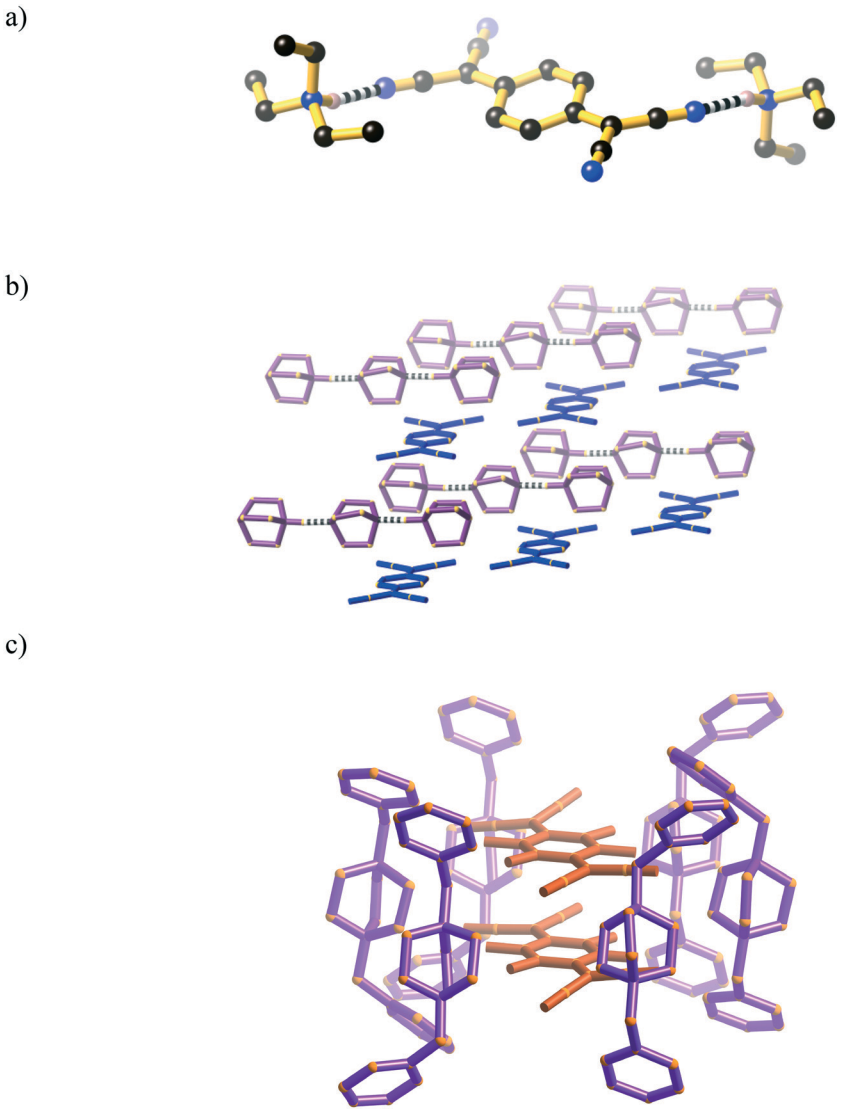

Fig. 18 a) Two $HNEt_3^+$ cations H-bonding to a $TCNQ^{2-}$ anion in $(HNEt_3)_2TCNQ$ (**93**). b) A view of $[(dabco{\cdot}H^+)_2(dabco)]TCNQ$ (**95**). The internally H-bonded $dabcoH^+$–dabco–$^+$Hdabco trimers (purple) interact electrostatically with strips of $TCNQ^{2-}$ anions (blue). c) The structure of dbdab–F_4-TCNQ (**96**) showing a pair of F_4TCNQ^{2-} units (orange) surrounded by dbdab cations (purple).

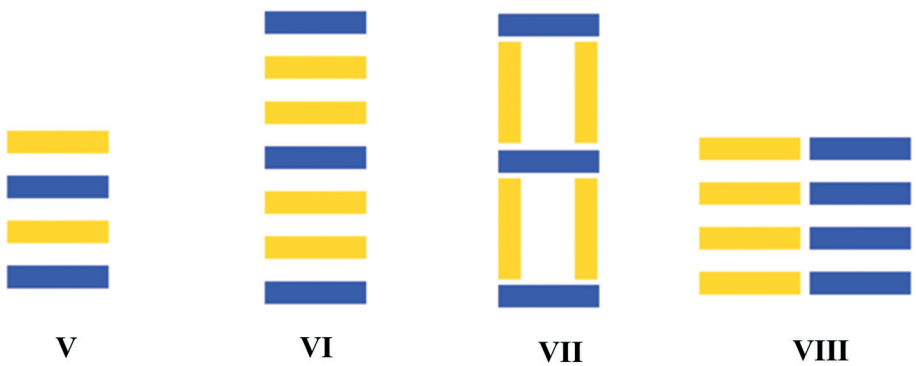

Fig. 19 The four packing arrangements of X_4TCNQ^{2-} anions (blue) and cations (yellow).

Confirmation of 2- charge

As a general rule, an increase in negative charge on X_4TCNQ^n (n = 0, −1 or −2) results in a shortening in b and d bond lengths whereas the c bond length increases (Scheme 2). The Kistenmacher equation, $q = A[c/(b + d)] + B$, where q is the estimated charge and A and B are coefficients, allows for an estimation of charge based upon the relevant bond lengths.[89]

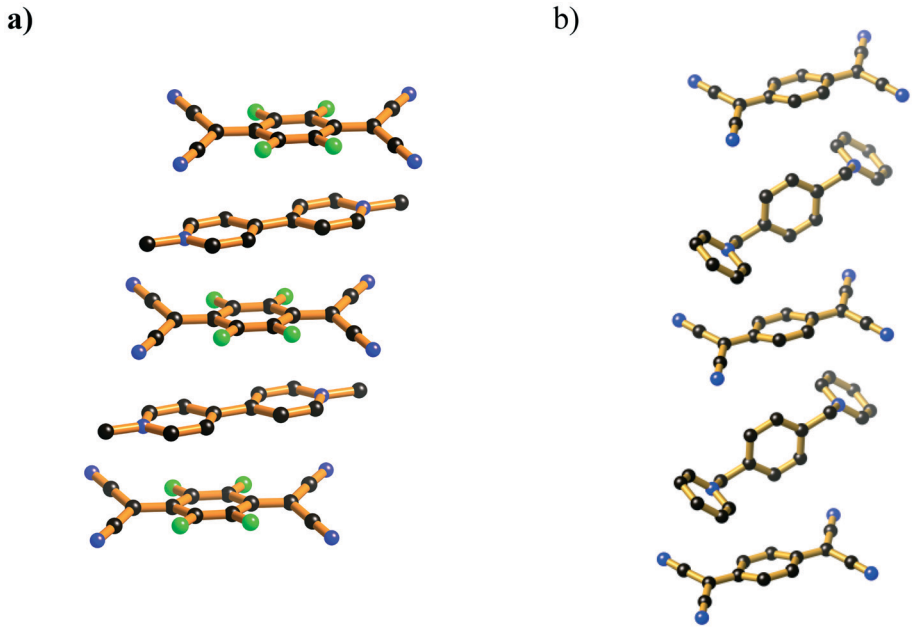

Fig. 20 A single type **V** stack in: a) (Mev)F_4TCNQ (**98**) and b) (dpx)TCNQ (**110**).

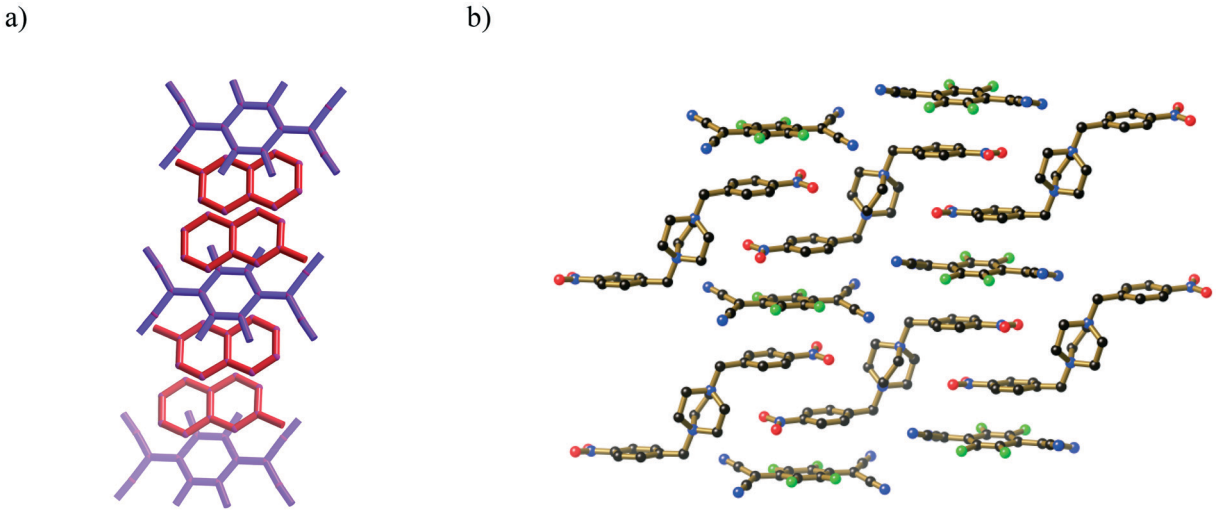

Fig. 21 a) A single type **VI** stack in (Meiq)$_2F_4$TCNQ (**114**), in which pairs of $Meiq^+$ cations (red) make face-to-face contacts with the F_4TCNQ^{2-} anions (purple). b) A view of the crystal packing of (dnbdab)F_4TCNQ (**116**) in which type **VI** stacks are linked by dnbdab cations.

Originally, the empirical values calculated for A and B were based on neutral and radical forms. We have now calculated revised values for A and B that take into account the dianionic form (for TCNQ A = −41.667, B = 19.818; for F_4-TCNQ A = −45.756, B = 21.846).[88] The IR nitrile stretches provide another indicator of the oxidation state, with an increase of charge resulting in a lowering of CN stretching frequencies (ν_{CN} stretching frequencies are typically in the range of 2170–2133 for F_4TCNQ^{2-} and 2176–2100 for $TCNQ^{2-}$).[90] Both methods have been used to confirm the 2- charge of the X_4-TCNQ moieties in the structures reported in this highlight. The estimated charge from the Kistenmacher relation are presented in Table 2.

Concluding remarks

The $TCNQ^{2-}$ and F_4TCNQ^{2-} dianions, obtained using the X_4TCNQH_2 synthetic approach, are versatile building blocks for the generation of a significant number of new supramolecular systems. A sizeable family of easily obtained, highly crystalline X_4TCNQ-based 1D, 2D and 3D coordination polymers and charge–transfer salts have been synthesised and structurally characterised. Whilst the choice of metal centre, counter-cation and reaction conditions all impact upon the type of structure obtained, the high variability in geometry and topology of X_4TCNQ^{2-} based coordination polymers can also be attributed to the variability in the binding of the dianion to metal centres;

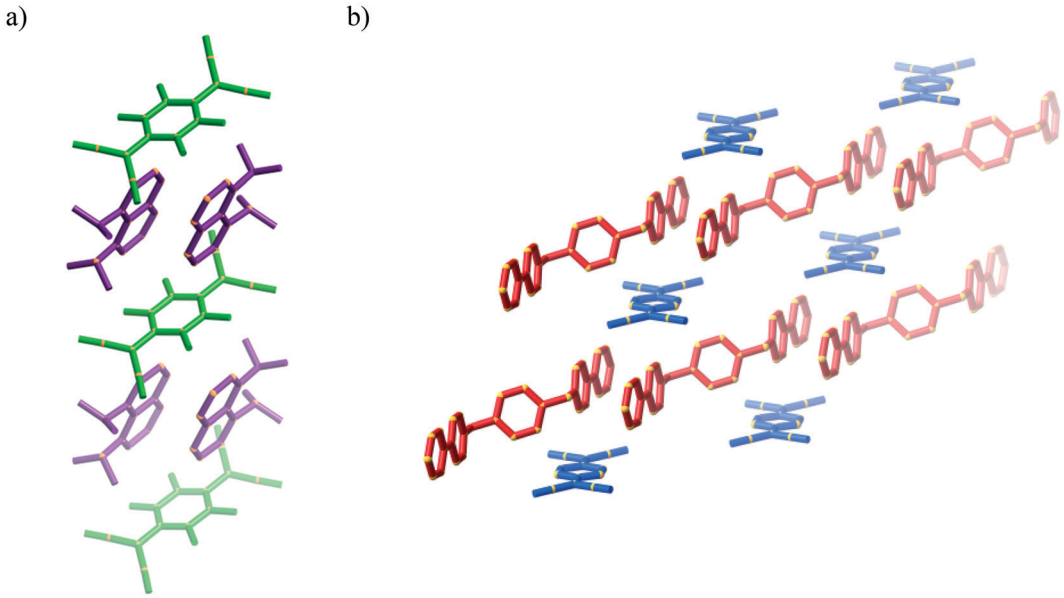

Fig. 22 a) A single type **VII** stack in (p-spongeH^{+})$_2$F$_4$TCNQ (**121**) in which pairs of cations (purple) make edge-to-face contact with the F$_4$TCNQ^{2-} anions (green). b) The type **VII** packing of (dbipx)F$_4$TCNQ (**124**) in which stacks are linked by the dications (red).

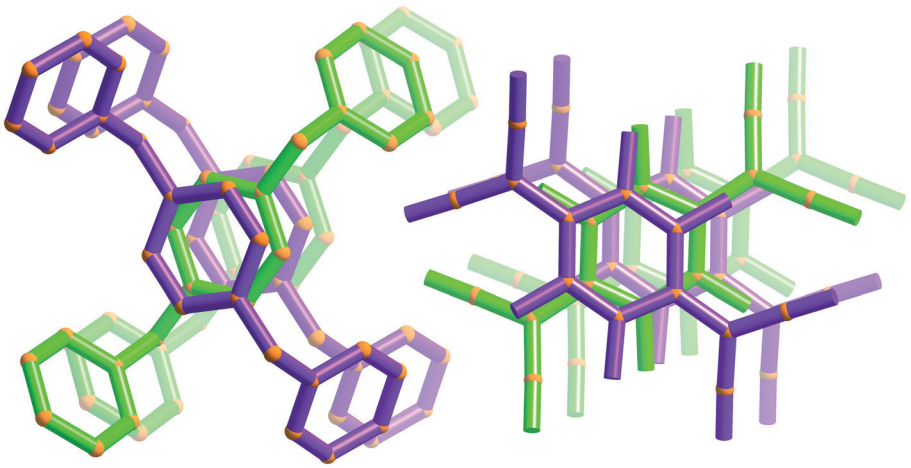

Fig. 23 The type **VIII** packing arrangement involving segregated stacks of dpx^{2+} cations and F$_4$TCNQ^{2-} anions in (dpx)F$_4$TCNQ (**125**).

X$_4$TCNQ dianions can bind to various numbers of metal centres, from 2 to 4 for the examples presented in the highlight. Furthermore, when acting as a ligand binding to four metal centres there is considerable variability in the location of the metal centres to which the dianions are bound. This is illustrated by the existence of both the square and rectangular arrangement of metal centres apparent in the type A and B geometries respectively (see Fig. 2). Inspection of these two contrasting structural types reveal relatively small deviations from linearity at the C–N–M angle can have a major influence on the type of structure obtained. Furthermore, the CN–C–CN moieties are able to rotate out of the plane of the C$_6$X$_4$ ring (Fig. 24) and as a consequence of this conformational flexibility, the four metal centres bound to an X$_4$TCNQ dianion are not required to be co-planar.

The combination of TCNQ and F$_4$TCNQ dianions with cations has led to the formation of several organic salts. In the case when accepting cations are employed, charge transfer complexes are formed, which result in intensely coloured crystals. The nature of the cation employed has been found to have a significant impact on the crystal packing arrangements.

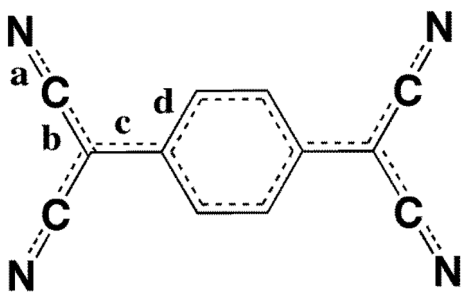

Scheme 2

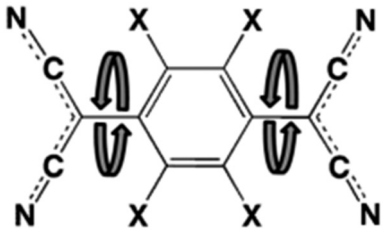

Fig. 24 A schematic representation highlighting the conformational flexibility associated with free rotation around the formally single C–C bonds of the X_4TCNQ dianion.

In many cases, contrary to the majority of radical derived compounds, open frameworks have been generated in which the X_4TCNQ^{2-} ligands are accessible. Such networks open up the very real possibility of generating redox active coordination polymers, *via* oxidative intercalation, in which some or all of the X_4TCNQ^n/X_4TCNQ^n moieties (n = 0 to −2) have been oxidised. Work in this area is currently ongoing.

Abbreviations

Ligands:

apyz	2-Aminopyrazine
2,2bipy	2,2′-Bipyridine
4,4bipy	4,4′-Bipyridine
DABCO	1,4-Diazabicyclo[2.2.2]octane
en	Ethylenediamine
Me_4en	*N*,*N*,*N*′*N*′-tetramethylethylenediamine
Me_2pyz	2,5-Dimethylpyrazine
phen	1,10-Phenanthroline
Obip	4,4′-Bipyridine-1,1′-dioxide
TACN	1,4,7-Triazacyclononane
tmpyz	2,3,5,6-Tetramethylpyrazine

Cations:

bv	Benzyl-viologen
dbdab	(Dibenzyl)dabco
dnbp	((3,5-Dinitro)benzyl)pyridinium
ddabx	(Didabco)xylene
diquat	1,1′-Ethylene-2,2′-bipyridylium
dcpx	Di-(4-cyanopyridinium)xylene
dnbdab	(Di-(4-nitrobenzyl))-dabco
dpbene	(Dipyridinium)butene
dpe	(Dipyridinium)ethane
dpicx	Di(picolinium)xylene
dbipx	Di-(4,4′-bipyridylium)xylene
dpmv	Diphenylmethane-viologen
dpx	(Dipyridinium)xylene
Etv	Ethyl-viologen
me_2dab	*N*,*N*′-dimethyldabco
Meiq	*N*-methyl-isoquinolinium
Mepyz	*N*-methyl-pyrazinium
Mev	Methyl-viologen
mnbiq	(*m*-Nitrobenzyl)isoquinolinium
mnbp	(*m*-Nitrobenzyl)pyridinium
Nspiro	1,1′-Spirobipiperidinium
phv	Phenylviologen
pnbphp	*p*-Nitrobenzyl-4-phenylpyridinium
pnpyz	(*p*-Nitrobenzyl)pyrazinium
p-spongeH^+	8-(Dimethylamino)-*N*,*N*-dimethylnaphthalen-1-ammonium

Conflicts of interest

There are no conflicts to declare.

Acknowledgements

The authors gratefully acknowledge the financial support of the Australian Research Council. A. L. S. and R. W. E. gratefully acknowledge the support of the Australian Government with respect to the provision of research scholarships. Several data collections were performed on the macromolecular crystallography beamlines at the Australian Synchrotron, Victoria, Australia.

References

1 R. P. Shibaeva and L. O. Atovmyan, *J. Struct. Chem.*, 1972, **13**, 514–531.
2 J. S. Pedersen and K. Carneiro, *Rep. Prog. Phys.*, 1987, **50**, 995–1043.
3 V. A. Starodub and T. N. Starodub, *Russ. Chem. Rev.*, 2014, **83**, 391–438.
4 M. J. Cohen, L. B. Coleman, A. F. Garito and A. J. Heeger, *Phys. Rev. B: Solid State*, 1974, **10**, 1298–1307.
5 P. W. Anderson, P. A. Lee and M. Saitoh, *Solid State Commun.*, 1973, **13**, 595–598.
6 J. Ferraris, D. O. Cowan, V. Walatka and J. H. Perlstein, *J. Am. Chem. Soc.*, 1973, **95**, 948–949.
7 F. H. Herbstein and M. Kapon, *Crystallogr. Rev.*, 2008, **14**, 3–74.
8 G. Saito and T. Murata, *Philos. Trans. R. Soc., A*, 2008, **366**, 139–150.
9 L. Shields, *J. Chem. Soc., Faraday Trans. 2*, 1985, **81**, 1.
10 R. A. Heintz, H. Zhao, X. Ouyang, G. Grandinetti, J. Cowen and K. R. Dunbar, *Inorg. Chem.*, 1999, **38**, 144–156.
11 Z. Gu, H. Wu, Y. Wei and J. Liu, *J. Phys. Chem.*, 1993, **97**, 2543–2545.
12 D. Y. Tu, C. S. Wang, Z. Y. Ji, W. P. Hu and M. Liu, in *IEEE Conference on Electron Devices and Solid-State Circuits*, IEEE, 2005, pp. 575–578.
13 R. S. Potember, T. O. Poehler, A. Rappa, D. O. Cowan and A. N. Bloch, *Synth. Met.*, 1982, **4**, 371–380.
14 S.-G. Liu, Y. Liu, P. Wu and D. Zhu, *Chem. Mater.*, 1996, **8**, 2779–2787.
15 R. Müller, S. De Jonge, K. Myny, D. J. Wouters, J. Genoe and P. Heremans, *Solid-State Electron.*, 2006, **50**, 601–605.
16 J. Billen, S. Steudel, R. Müller, J. Genoe and P. Heremans, *Appl. Phys. Lett.*, 2007, **91**, 263507.
17 T. Oyamada, H. Tanaka, K. Matsushige, H. Sasabe and C. Adachi, *Appl. Phys. Lett.*, 2003, **83**, 1252.

18 H. Liu, Q. Zhao, Y. Li, Y. Liu, F. Lu, J. Zhuang, S. Wang, L. Jiang, D. Zhu, D. Yu and L. Chi, *J. Am. Chem. Soc.*, 2005, **127**, 1120–1121.
19 C. Ouyang, Y. Guo, H. Liu, Y. Zhao, G. Li, Y. Li, Y. Song and Y. Li, *J. Phys. Chem. C*, 2009, **113**, 7044–7051.
20 H. Liu, Z. Liu, X. Qian, Y. Guo, S. Cui, L. Sun, Y. Song, Y. Li and D. Zhu, *Cryst. Growth Des.*, 2010, **10**, 237–243.
21 R. C. Hoffman and R. S. Potember, *Appl. Opt.*, 1989, **28**, 1417–1421.
22 R. S. Potember, T. O. Poehler and R. C. Benson, *Appl. Phys. Lett.*, 1982, **41**, 548.
23 H. Hoshino, S. Matsushita and H. Samura, *Jpn. J. Appl. Phys.*, 1986, **25**, L341–L342.
24 H. Wu-Qiao, W. Yi-Qun, G. Dong-Hong and G. Fu-Xi, *Chin. Phys. Lett.*, 2003, **20**, 2178–2181.
25 D. G. Humphrey, G. D. Fallon and K. S. Murray, *J. Chem. Soc., Chem. Commun.*, 1988, 1356–1358.
26 M. C. Grossel, F. A. Evans, J. A. Hriljac, J. R. Morton, Y. Lepage, K. F. Preston, L. H. Sutcliffe and A. J. Williams, *J. Chem. Soc., Chem. Commun.*, 1990, 439.
27 M. C. Grossel, F. A. Evans, J. A. Hriljac, K. Prout and S. C. Weston, *J. Chem. Soc., Chem. Commun.*, 1990, 1494.
28 L. Ballester, M. C. Barral, A. Gutiérrez, R. Jimenez-Aparicio, J. M. Martinez-Muyo, M. F. Perpiñán, M. A. Monge and C. Ruiz-Valero, *J. Chem. Soc., Chem. Commun.*, 1991, **80**, 1396.
29 L. Stuart, L. Bartley and K. R. Dunbar, *Angew. Chem., Int. Ed. Engl.*, 1991, **30**, 448–450.
30 M. C. Grossel and S. C. Weston, *J. Chem. Soc., Chem. Commun.*, 1992, 1510.
31 J. P. Cornelissen, J. H. Van Diemen, L. R. Groeneveld, J. G. Haasnoot, A. L. Spek and J. Reedijk, *Inorg. Chem.*, 1992, **31**, 198–202.
32 P. J. Kunkeler, P. J. van Koningsbruggen, J. P. Cornelissen, A. N. van der Horst, A. M. van der Kraan, A. L. Spek, J. G. Haasnoot and J. Reedijk, *J. Am. Chem. Soc.*, 1996, **118**, 2190–2197.
33 M. T. Azcondo, L. Ballester, A. Gutiérrez, M. F. Perpiñán, U. Amador, C. Ruiz-Valero and C. Bellitto, *J. Chem. Soc., Dalton Trans.*, 1996, 3015.
34 L. Ballester, A. M. Gil, A. Gutiérrez, M. F. Perpiñán, M. T. Azcondo, A. E. Sánchez, U. Amador, J. Campo and F. Palacio, *Inorg. Chem.*, 1997, **36**, 5291–5298.
35 D. Fortin, M. Drouin, P. D. Harvey, F. G. Herring, D. A. Summers and R. C. Thompson, *Inorg. Chem.*, 1999, **2**, 1253–1260.
36 H. Hartmann, W. Kaim, I. Hartenbach, T. Schleid, M. Wanner and J. Fiedler, *Angew. Chem., Int. Ed.*, 2001, **40**, 2842–2844.
37 L. Ballester, A. M. Gil, A. Gutiérrez, M. F. Perpiñán, M. T. Azcondo, A. E. Sánchez, C. Marzin, G. Tarrago and C. Bellito, *Chem. – Eur. J.*, 2002, **8**, 2539–2548.
38 A. N. Maity, B. Sarkar, M. Niemeyer, M. Sieger, C. Duboc, S. Zalis and W. Kaim, *Dalton Trans.*, 2008, 5749.
39 C. Campana, K. R. Dunbar and X. Ouyang, *Chem. Commun.*, 1996, 2427.
40 H. Zhao, R. A. Heintz, K. R. Dunbar and R. D. Rogers, *J. Am. Chem. Soc.*, 1996, **118**, 12844–12845.
41 P. G. Lacroix and J. Daran, *J. Chem. Soc., Dalton Trans.*, 1997, 1369–1374.
42 H. Miyasaka, C. S. Campos-Fernández, R. Clérac and K. R. Dunbar, *Angew. Chem., Int. Ed.*, 2000, **39**, 3831–3835.
43 H. Zhao, R. A. Heintz, X. Ouyang, K. R. Dunbar, C. F. Campana and R. D. Rogers, *Chem. Mater.*, 1999, **11**, 736–746.
44 M. T. Johnson, A. M. Arif and J. S. Miller, *Eur. J. Inorg. Chem.*, 2000, **2000**, 1781–1787.
45 H. Zhao, M. J. Bazile, J. R. Galán-Mascarós and K. R. Dunbar, *Angew. Chem., Int. Ed.*, 2003, **42**, 1015–1018.
46 H. Miyasaka, T. Izawa, N. Takahashi, M. Yamashita and K. R. Dunbar, *J. Am. Chem. Soc.*, 2006, **128**, 11358–11359.
47 H. Miyasaka, T. Madanbashi, K. Sugimoto, Y. Nakazawa, W. Wernsdorfer, K. I. Sugiura, M. Yamashita, C. Coulon and R. Clérac, *Chem. – Eur. J.*, 2006, **12**, 7028–7040.
48 Y. Q. Song, Q. Y. Lv, S. Z. Zhan, J. G. Wang, J. Y. Su and A. Ding, *Inorg. Chem. Commun.*, 2008, **11**, 672–674.
49 Y. L. Bai, J. Tao, R. Bin Huang and L. S. Zheng, *Angew. Chem., Int. Ed.*, 2008, **47**, 5344–5347.
50 C. Avendano, Z. Zhang, A. Ota, H. Zhao and K. R. Dunbar, *Angew. Chem., Int. Ed.*, 2011, **50**, 6543–6547.
51 M. Ballesteros-Rivas, A. Ota, E. Reinheimer, A. Prosvirin, J. Valdés-Martinez and K. R. Dunbar, *Angew. Chem., Int. Ed.*, 2011, **50**, 9703–9707.
52 M. Ballesteros-Rivas, H. Zhao, A. Prosvirin, E. W. Reinheimer, R. a. Toscano, J. Valdés-Martínez and K. R. Dunbar, *Angew. Chem., Int. Ed.*, 2012, **51**, 5124–5128.
53 Z. Zhang, H. Zhao, H. Kojima, T. Mori and K. R. Dunbar, *Chem. – Eur. J.*, 2013, **19**, 3348–3357.
54 E. Shurdha, C. E. Moore, A. L. Rheingold, S. H. Lapidus, P. W. Stephens, A. M. Arif and J. S. Miller, *Inorg. Chem.*, 2013, **52**, 10583–10594.
55 Q. Li, P. Yan, G. Hou, Y. Wang and G. Li, *Dalton Trans.*, 2013, **42**, 7810.
56 Q. Li, Y. Wang, P. Yan, G. Hou and G. Li, *Inorg. Chim. Acta*, 2014, **413**, 32–37.
57 M.-K. Kim, Y.-I. Kim, S. B. Moon and S.-N. Choi, *Bull. Korean Chem. Soc.*, 1996, **17**, 424.
58 K. I. Pokhodnya, N. Petersen and J. S. Miller, *Inorg. Chem.*, 2002, **41**, 1996–1997.
59 R. Clérac, S. O'Kane, J. Cowen, X. Ouyang, R. Heintz, H. Zhao, M. J. Bazile and K. R. Dunbar, *Chem. Mater.*, 2003, **15**, 1840–1850.
60 E. B. Vickers, T. D. Selby, M. S. Thorum, M. L. Taliaferro and J. S. Miller, *Inorg. Chem.*, 2004, **43**, 6414–6420.
61 E. B. Vickers, I. D. Giles and J. S. Miller, *Chem. Mater.*, 2005, **17**, 1667–1672.
62 A. Nafady, A. P. O'Mullane, A. M. Bond and A. K. Neufeld, *Chem. Mater.*, 2006, **18**, 4375–4384.
63 A. Nafady, A. M. Bond, A. Bilyk, A. R. Harris, A. I. Bhatt, A. P. O'Mullane and R. De Marco, *J. Am. Chem. Soc.*, 2007, **129**, 2369–2382.
64 A. Nafady and A. M. Bond, *Inorg. Chem.*, 2007, **46**, 4128–4137.
65 X. Qu, A. Nafady, A. Mechler, J. Zhang, A. R. Harris, A. P. O'Mullane, L. L. Martin and A. M. Bond, *J. Solid State Electrochem.*, 2008, **12**, 739–746.

66 A. Nafady, A. M. Bond and A. Bilyk, *J. Phys. Chem. C*, 2008, **112**, 6700–6709.
67 A. R. Siedle, G. A. Candela and T. F. Finnegan, *Inorg. Chim. Acta*, 1979, **35**, 125–130.
68 R. Choukroun, C. Lorber, D. De Caro and L. Vendier, *Organometallics*, 2006, **25**, 4243–4246.
69 S. Shimomura, R. Matsuda, T. Tsujino, T. Kawamura and S. Kitagawa, *J. Am. Chem. Soc.*, 2006, **128**, 16416–16417.
70 N. Lopez, H. Zhao, A. V. Prosvirin, A. Chouai, M. Shatruk and K. R. Dunbar, *Chem. Commun.*, 2007, 4611.
71 J. S. Miller, J. H. Zhang, W. M. Reiff, D. A. Dixon, L. D. Preston, A. H. Reis, E. Gebert, M. Extine and J. Troup, *et al.*, *J. Phys. Chem.*, 1987, **91**, 4344–4360.
72 M. Moscherosch and W. Kaim, *Inorg. Chim. Acta*, 1993, **206**, 229–230.
73 H. Oshio, E. Ino, T. Ito and Y. Maeda, *Bull. Chem. Soc. Jpn.*, 1995, **68**, 889–897.
74 T. H. Le, A. Nafady, X. Qu, L. L. Martin and A. M. Bond, *Anal. Chem.*, 2011, **83**, 6731–6737.
75 B. F. Abrahams, T. A. Hudson and R. Robson, *Cryst. Growth Des.*, 2008, **8**, 1123–1125.
76 M. R. Suchanski and R. P. Van Duyne, *J. Am. Chem. Soc.*, 1976, **98**, 250–252.
77 X. Zhang, Z. Zhang, H. Zhao, J.-G. Mao and K. R. Dunbar, *Chem. Commun.*, 2014, **50**, 1429–1431.
78 B. F. Abrahams, R. W. Elliott, T. A. Hudson and R. Robson, *Cryst. Growth Des.*, 2010, **10**, 2860–2862.
79 B. F. Abrahams, R. W. Elliott and R. Robson, *Aust. J. Chem.*, 2014, **67**, 1871.
80 S. Shimomura, N. Yanai, R. Matsuda and S. Kitagawa, *Inorg. Chem.*, 2011, **50**, 172–177.
81 X. Zhang, M. R. Saber, A. P. Prosvirin, J. H. Reibenspies, L. Sun, M. Ballesteros-Rivas, H. Zhao and K. R. Dunbar, *Inorg. Chem. Front.*, 2015, **2**, 904–911.
82 T. Le, A. Nafady, N. Vo, R. Elliott, T. A. Hudson, R. Robson, B. F. Abrahams, L. L. Martin and A. M. Bond, *Inorg. Chem.*, 2014, **53**, 3230–3242.
83 B. F. Abrahams, R. W. Elliott, T. A. Hudson, R. Robson and A. L. Sutton, *Cryst. Growth Des.*, 2015, **15**, 2437–2444.
84 M. R. Saber, A. V. Prosvirin, B. F. Abrahams, R. W. Elliott, R. Robson and K. R. Dunbar, *Chem. – Eur. J.*, 2014, **20**, 7593–7597.
85 B. F. Abrahams, R. W. Elliott, T. A. Hudson and R. Robson, *CrystEngComm*, 2012, **14**, 351.
86 B. F. Abrahams, R. W. Elliott, T. A. Hudson and R. Robson, *Cryst. Growth Des.*, 2013, **13**, 3018–3027.
87 T. A. Hudson and R. Robson, *Cryst. Growth Des.*, 2009, **9**, 1658–1662.
88 A. L. Sutton, B. F. Abrahams, D. M. D'Alessandro, R. W. Elliott, T. A. Hudson, R. Robson and P. M. Usov, *CrystEngComm*, 2014, **16**, 5234.
89 T. J. Kistenmacher, T. J. Emge, A. N. Bloch and D. O. Cowan, *Acta Crystallogr., Sect. B: Struct. Crystallogr. Cryst. Chem.*, 1982, **38**, 1193–1199.
90 J. S. Chappell, A. N. Bloch, W. a Bryden, M. Maxfield, T. O. Poehler and D. O. Cowan, *J. Am. Chem. Soc.*, 1981, **103**, 2442–2443.

